



International Civil Aviation Organization

**The Sixteenth Meeting of the Regional Airspace Safety Monitoring  
Advisory Group (RASMAG/16)**

Bangkok, Thailand, 20 – 24 February 2012

---

**Agenda Item 3: Reports from Asia/Pacific RMAs and EMAs**

**AIRSPACE ANALYSIS OF BAY OF BENGAL ARABIAN SEA INDIAN OCEAN REGION  
AND  
SAFETY ASSESSMENT OF RNP10 ROUTES**

**L301, L507, L509, L510, L759, M300, M770, N563, N571, N877, N895, P570, P574, P628, P646 and P762**

(Presented by BOBASMA)

**SUMMARY**

This paper presents a revised Airspace Analysis of Bay of Bengal Arabian Sea Indian Ocean region and Safety Assessment for the continued safe use of 50NM Reduced Longitudinal separation on RNP10 routes L301, L507, L509, L510, L759, M300, M770, N563, N571, N87, N895, P570, P574, P628, P646 and P762.

The qualitative Risk Assessment for the lateral and longitudinal collision risk has been carried out using internationally recognized Reich Collision Risk Model. The Safety assessment was conducted using the Traffic Sample Data of December 2011, radar surveillance data from all ATC centres and GNE data collected from 1st July 2010 to 31st December 2011.

This paper relates to –

**Strategic Objectives:**

- A: *Safety – Enhance global civil aviation safety*
- C: *Environmental Protection and Sustainable Development of Air Transport – Foster harmonized and economically viable development of international civil aviation that does not unduly harm the environment*

**Global Plan Initiatives:**

- GPI-8 Collaborative airspace design and management
- GPI-9 Situational awareness
- GPI-21 Navigation systems
- GPI-22 Communication infrastructure

## 1. INTRODUCTION

- 1.1 The Bay Of Bengal Reduced Horizontal Separation Task Force in its 6<sup>th</sup> meeting in September 2011 decided on a “Go decision” for the Phase2 implementation of 50NM Reduced Longitudinal Separation in the Bay of Bengal Arabian Sea airspace and formulated an “Implementation Readiness Plan”. The meeting also required that BOBASMA conduct the pre- implementation Safety Assessment for the routes L301, L507, L509, L510, L759, M300, M770, N563, N877, N895, P570, P574, P628 and P646 and forward it to ICAO – APAC. BOBASMA conducted the Airspace analysis and Safety assessment using TSD of August 2011. The lateral collision risk was estimated to be  $0.760904 \times 10^{-9}$  and the longitudinal collision risk  $3.1759 \times 10^{-9}$ . The report was forwarded to SEASMA & AAMA who are the mentors for BOBASMA for a period of twelve months for peer review as per decision 22/14 of the 22<sup>nd</sup> meeting of APANPIRG held in September 2011. After peer review both SEASMA and AAMA endorsed the methodology used, and the risk estimates arrived at. The report was accepted by ICAO-APAC.
- 1.2 The present Safety Assessment and Airspace Analysis have been conducted using Traffic Sample Data of December 2011, including Phase2B & Phase2C routes. The final Safety Assessment and the Airspace analysis report was submitted to the mentors SEASMA and AMA for peer review. The peer group has endorsed the methodology adopted by BOBASMA in arriving at the risk estimates except for a few changes recommended in the definition of  $P_y(0)$  &  $P_z(0)$  and some editorial changes in the report. BOBASMA has incorporated the changes in the Working Paper. The Airspace analysis is attached as Appendix – A and Safety Assessment as Appendix – B to this paper.

## 2. OBJECTIVE

The Safety Assessment and Airspace Analysis have been conducted with the objective to confirm that the regionally established Target Level of Safety for the airspace has been met for the introduction of 50 NM RLS on Phase2C routes M300 and P570 and the continued safe use of RLS 50NM on Phase-1, 2A and 2B routes.

## 3. DISCUSSION

### 3.1. Phase1 and Phase2 RHS Implementation.

Reduced horizontal separation was implemented in Phase1 along two routes N571 & P762 and in Phase2 along fourteen routes, L301, L507, L509, L510, L759, M300, M770, N563, N877, N895, P570, P574, P628 & P646. However Phase1 witnessed not many aircraft pairs with RLS due to various constraints which restricted implementation on N571 and there was no opportunity for using 50NM RLS on low density route P762 till date.

In Phase2 since Muscat was not willing to accept aircraft pairs with 50NM RLS Mumbai ACC had to restrict implementation of RLS for westbound traffic entering Muscat ACC. Muscat was party to the “GO” decision taken in the BOB-RHS/TF6 meeting, in September 2011, for implementation of RHS on Phase2 routes. The LOA between Muscat and Mumbai was also signed. Non participation by Muscat has affected implementation of RHS on routes L301, N571, P574, N563, M300 and P570. Delayed implementation by member states in the East also affected the number of aircraft pairs that could be provided with 50NM RLS. There has been no instance of westbound aircraft pairs with 50 NM RLS entering either Chennai or Kolkata airspace from the east during the initial observation period from 15<sup>th</sup> to 31<sup>st</sup> December 2011. It is observed that full

benefits of implementation of 50 NM RLS cannot be realized until after implementation of Phase2C and states such as Muscat which are adjacent to BOBASIO region also implement 50 NM RLS.

### 3.2 Data link capability.

A sample study conducted in Chennai FIR using seven days data from 25<sup>th</sup> to 31<sup>st</sup> December 2011 showed that there is a considerable increase (69%) of the aircraft population having data link capability, however it is observed that only 88% of the above population had actually logged on to ADS/CPDLC. Figure1 below shows the percentage of data link capable aircraft that were not logging on to data link during the seven days for which data was collected. As data link is the primary means of communication over Oceanic airspace more aircraft need to be data link capable to derive maximum benefit of RHS implementation.

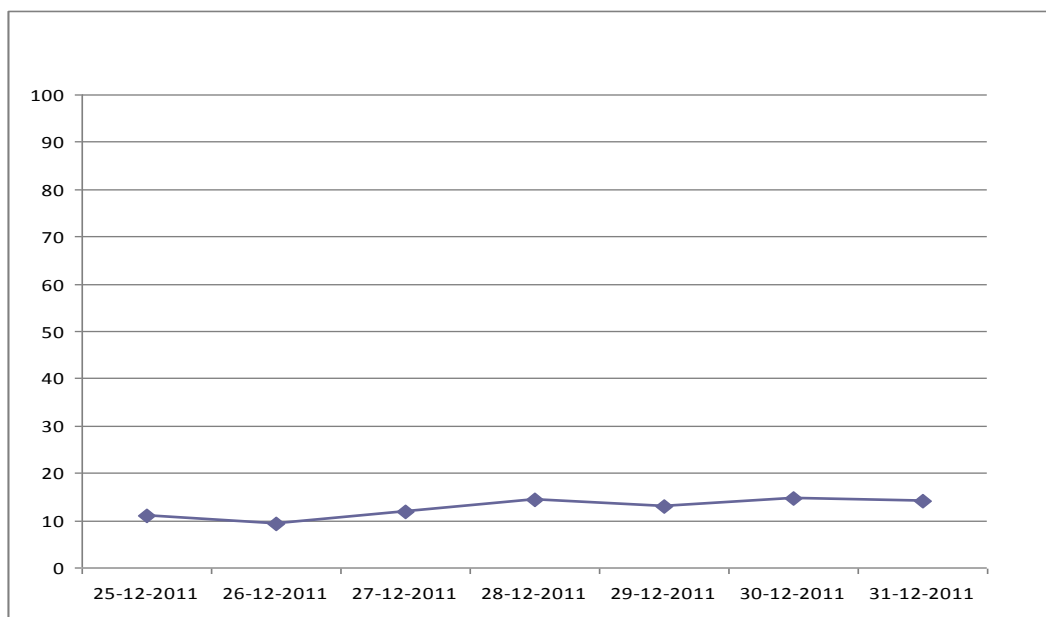


**Figure1. Percentage of data link capable aircraft not logged on.**

ATS interoperability tests were conducted twice between Chennai and Kuala Lumpur in December 2011 and January 2012, selected messages reflecting normal ATC operations including Handoff and NDA messages were exchanged successfully between the two ATSU's. The same test was conducted between Chennai and Colombo in April 2011. However as Colombo ground system was not capable of automatic Hand-offs the virtual aircraft had to log off with Chennai and then re log in with Colombo. The test between Chennai and Mumbai in August 2011 failed due to issues in the New ATM Automation system at Chennai and this has subsequently been rectified.

### 3.3 Database of PBN Approvals.

The website for BOBASMA was established and also demonstrated during the last RASMAG meeting in August 2011. Member states were informed about the availability of direct access for uploading of data. The relevant forms, EMA A1, A2, & A3 from the EMA Handbook had been sent to the member states. States were requested to forward the POC detail at the earliest so that BOBASMA can issue a onetime user id and password. However till date BOBASMA is not in receipt of the Point of Contact detail of any member state and as such the data on the website could not be updated. Efforts are being taken to directly contact the relevant authorities of member states by all means of communication available. Pending receipt of POC detail, requests for State PBN approval

data has been sent directly to the state authorities. Member states have committed to provide the data at the earliest.

**3.4 Data on Gross Navigational Error and Traffic Sample Data.**

It was decided in BOB-RHS/TF6 meeting to dispense with the requirement of member states to sign a Letter of Agreement with the EMA as many states had internal administrative issues in signing agreements with foreign entities. Alternately a procedure for sharing of data was outlined in the report of the meeting. However the TSD to be sent to BOBASMA was not received from many states in time for the conduct of this Safety assessment. The TSD from Pakistan and Afghanistan was received late and hence could not be included in the present study. BOBASMA intends to conduct a separate Safety Assessment using the TSD of December 2011 of Delhi, Karachi, Lahore and Kabul FIR by the end of February 2012.

**3.5 Implementation of RHS on L333 and M875.**

During BOB-RHS/TF6 meeting routes M875 and L333 were not considered for implementation of 50 NM RLS. But as India and Pakistan plan to introduce 50 NM RLS on these two routes, the two routes have been included in the Airspace Analysis. It is evident from the analysis, that availability of contiguous VHF and Radar coverage, as shown in Figure 2 & 3, may even permit application of 10NM Radar separation. However considering other factors like radar redundancy, radar Hand-off and AIDC interoperability issues, to begin with India and Pakistan may safely introduce 50 NM RLS on these two routes using VHF DCPC and radar surveillance. This would enhance a harmonized transition of aircraft pairs with RLS at the TCPs between India and Pakistan. Accordingly India and Pakistan propose to implement 50NM RLS on these routes by end February 2012.

3.6 The Lateral collision risk is estimated to be  $1.04405 \times 10^{-9}$  & the Longitudinal collision risk  $0.67326 \times 10^{-9}$ , both of which are below the TLS of  $5 \times 10^{-9}$ . Thus it can be concluded that the Safety Assessment supports the introduction of 50 NM RLS in Phase 2C routes and the continued safe use of 50NM RLS on Phase-1 & 2 routes.

**4. ACTION BY THE MEETING.**

The meeting is invited to:

- a. Note the estimated lateral and longitudinal collision risk which supports the continued safe use of 50 NM RLS on Phase1 & 2 routes
- b. Take note of the difficulty faced by Mumbai due to non participation by Muscat in the implementation.
- c. Impress airline operators the need to equip data link capability on long haul flights and also to logon when equipped with the ground stations as appropriate.
- d. Urge member states to provide GNE and TSD to BOBASMA.
- e. Urge member states to provide En route PBN or Data link approvals.
- f. Note the airspace analysis for the implementation of 50NM RHS on L333 and M875.

.....

**Appendix - A****BOBASIO AIRSPACE ANALYSIS****A revised analysis of the traffic flow, Aircraft and Operators in the****Bay of Bengal Arabian Sea, Indian Ocean Region.****1. Introduction**

- 1.1 The Bay of Bengal Arabian Sea Indian Ocean route system comprises of near parallel RNP10 routes which are part of the EMARSSH (Asia to Middle East/Europe Route Structure South of Himalayas) project introduced in November 2002. RVSM was introduced on these routes from November 2003.
- 1.2 With increasing demands for optimum flight level by aircraft operators, the need to reduce fuel cost, and reduce emissions it has become imperative to make full use of the existing aircraft capability and available ground infrastructure to enhance capacity.
- 1.3 It has been felt for long, that opportunity exists for increasing capacity and efficiency within the present route network by reducing the longitudinal separation applicable between pairs of suitably equipped aircraft.

**2. Background**

BBACG established the Bay Of Bengal Reduced Horizontal Separation TASK Force (BOB-RHS/TF) in January 2009 to implement RHS 50NM Longitudinal in the Bay of Bengal Arabian Sea region. As mandated by the BOB-RHS Task Force, RHS 50NM longitudinal was implemented on two routes N571 & P762 in Phase 1 from 30<sup>th</sup> June 2011. In Phase 2, based on the “Implementation Readiness Plan” of BOB-RHS/TF/6 meeting, India, Malaysia, Thailand, Muscat, Myanmar and Pakistan introduced Reduced Longitudinal Separation of 50NM on RNP10 routes P628, L510, N877, L759, M770, L301, N895, P646, L507, L509, P574, N563, M300 and P570 from 15<sup>th</sup> December 2011. Indonesia implemented RLS from 12<sup>th</sup> January 2012 and Sri Lanka will start implementation from 8<sup>th</sup> March 2012

**3. Purpose**

This Know Your Airspace Analysis of the BOBASIO region is intended to give detailed information on the route structure, usage of the different ATS routes, issues involved when routes transit from one state to another, major operator and airframes that operate in the region and describe the general traffic flow. The post implementation study, conducted using data from 15<sup>th</sup> December 2011 to 31<sup>st</sup> December 2011, outlines the number of aircraft pairs provided with 50NM RLS within the three Indian FIRs.

**4. Data Collection**

Table1 below shows the record of TSD of December 2011, received from the different Flight Information Regions. The sixteen RNP10 Routes on which 50NM RLS was implemented in the Bay of Bengal Arabian Sea Indian Ocean region, in the first two phases and routes L333 & M875 has been taken up for this study.

S.No	FIR/ACC	Received	Remarks
01	Chennai	Yes	
02	Mumbai	Yes	
03	Kolkata	Yes	
04	Delhi	Yes	
05	Colombo	Yes	
06	Kualalumpur	Yes	Incomplete
07	Jakarta	No	
08	Myanmar	No	
09	Bangkok	Yes	
10	Male	No	
11	Lahore	No	
12	Karachi	No	
13	Kabul	No	

Table 1. Record of TSD of December 2011

## 5. Airspace Description

The Bay of Bengal Arabian Sea Indian Ocean airspace comprises primarily of RNP10 routes spaced 50NM laterally connecting airports in South East Asia to that in India, Middle East and Europe. The major traffic flows in the Bay of Bengal Arabian Sea Indian Ocean airspace is shown in Figure1.

### 5.1 Arabian Sea Airspace:

The Arabian Sea airspace which falls under Mumbai FIR has ATS routes primarily from Middle East to India and beyond towards South East Asia. Two routes connect Middle East to Male. In addition there are few crossing routes that connect Africa & Mauritius to India. A Flight Level Allocation Scheme (FLAS) wherein FL300 and FL330 are reserved for the four crossing routes is being followed while allocating levels for aircraft. The FLAS is suspended between 0530 UTC to 0930 UTC to facilitate higher levels for long haul flights from Middle East Asia to Australia. L301 is the most used RNP10 route.

- 5.1.1 Reduced Longitudinal Separation of 50NM is applicable between suitably equipped aircraft on L301, M300, N571, N563, P574, & P570 in addition to the existing 10 min or 80NM longitudinal separation. On all other routes only 10 min or 80NM longitudinal separation is applicable. A longitudinal separation of 15 min is prescribed for crossing tracks.

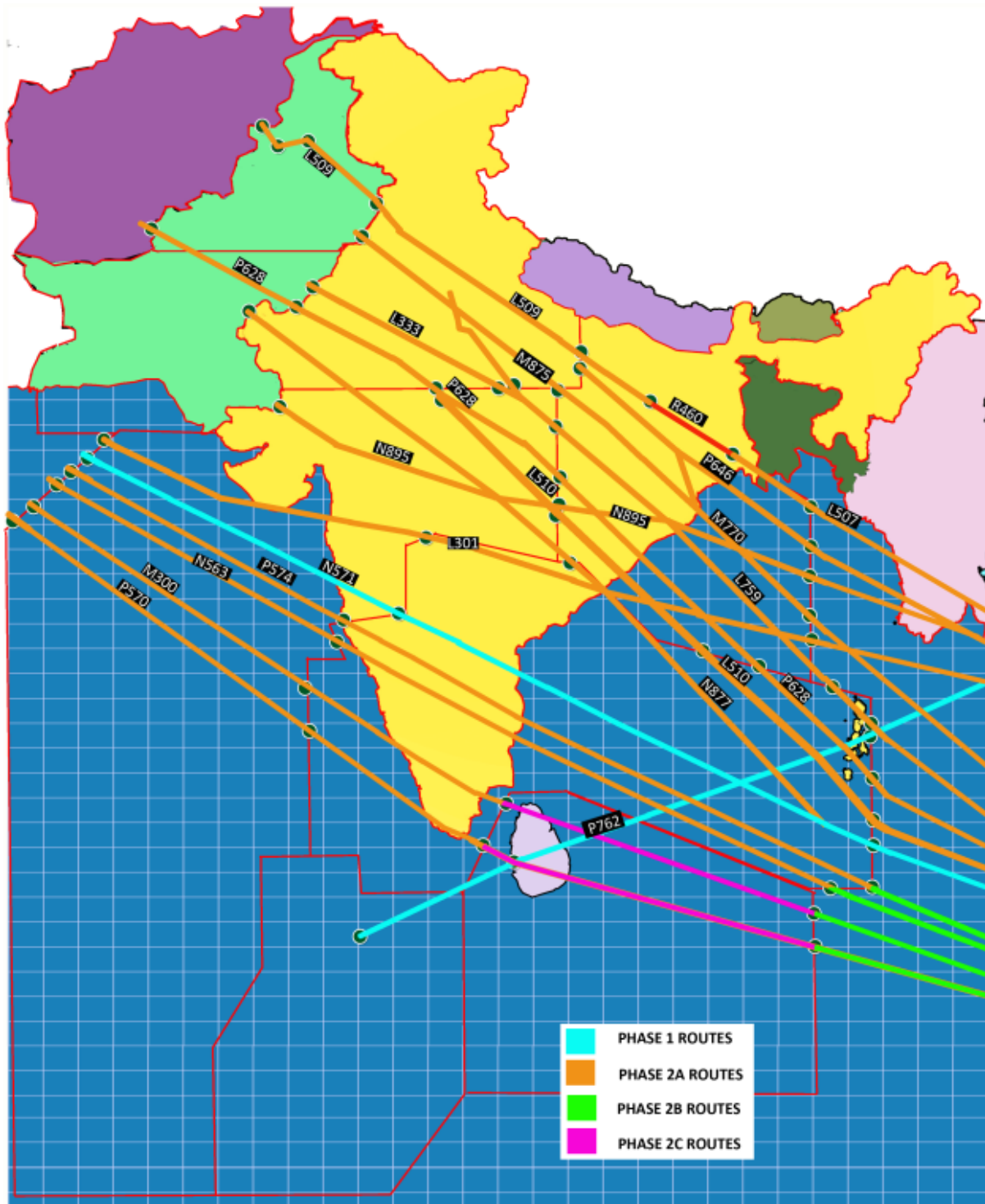


Figure1. RHS Routes Map.

## 5.2 Bay of Bengal Airspace

The Bay of Bengal airspace serves the traffic flying into/from the busy airports of South East Asia, Japan and Australia. Two sets of RNP10 routes originating from South East Asia proceed towards Middle East and Europe. Crossing route P762 from Bangkok Colombo/South Africa crosses all the other RNP10 routes. FL290 and FL320 have been allotted as No PDC level on P762. Converging route P761 from Chennai crosses N877, L510 and converges with P628 over Port Blair.

5.3 Restrictions and Procedures

The applicable restrictions and procedures on the RNP10 routes are given in Table2.

RNP10 Route	Restrictions and Procedures.
L301	i)segment BUSBO – AAU – NOBAT not available from 0030UTC to 1300UTC. Aircraft operating outside these times should follow L505 between BUSBO to NOBAT. ii) Restrictions are also imposed whenever Danger Area VED73 is active.
L509	Route available between 1630 UTC to 2230 UTC
L510	Route will be EAST bound between 1500 UTC at GIVAL and 2230 UTC at IBANI , ATC can re-route west bound flights also at FL360,FL340,FL300 & FL280
L759	Route bidirectional between AGRA VOR and MIPAK
M770	i)Route from BUBKO- JJS is available only between 1630 UTC to 2230 UTC ii) Outside these times aircraft to route via M773
N563	i)Route from LEKAP in the east to KAKIB in the west is not available from 0030 UTC to 1630 UTC. ii) Route segment MEPAK to REXOD available H24
N877	Restrictions are imposed when VED 73 is active
P570	Route unidirectional between BASUR to TVM
P628	Route Bidirectional between IBANI - VIKIT
P646	i)Route from DOPID to JJS available between only between 1630 UTC to 2330 UTC ii)outside these times aircraft to route via DOPID to CEA

Table2. Applicable Restrictions and Procedures.

5.4 Figure2 & 3 depicts the extent of Radar and VHF coverage available over the continental airspace of India.

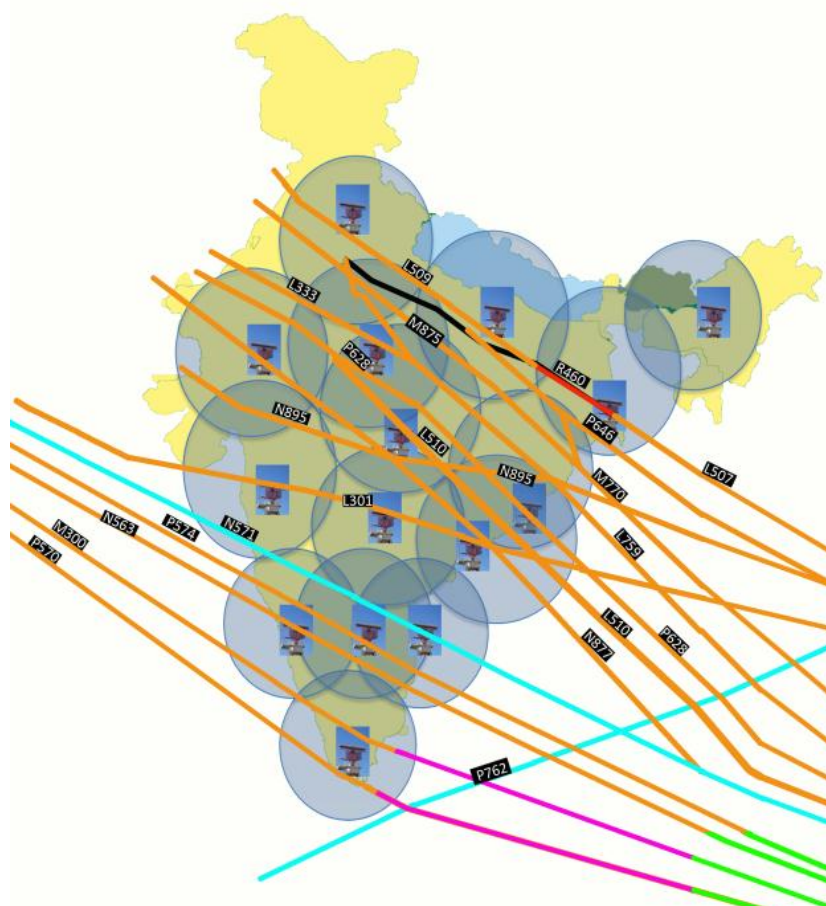


Figure2. Radar coverage map.



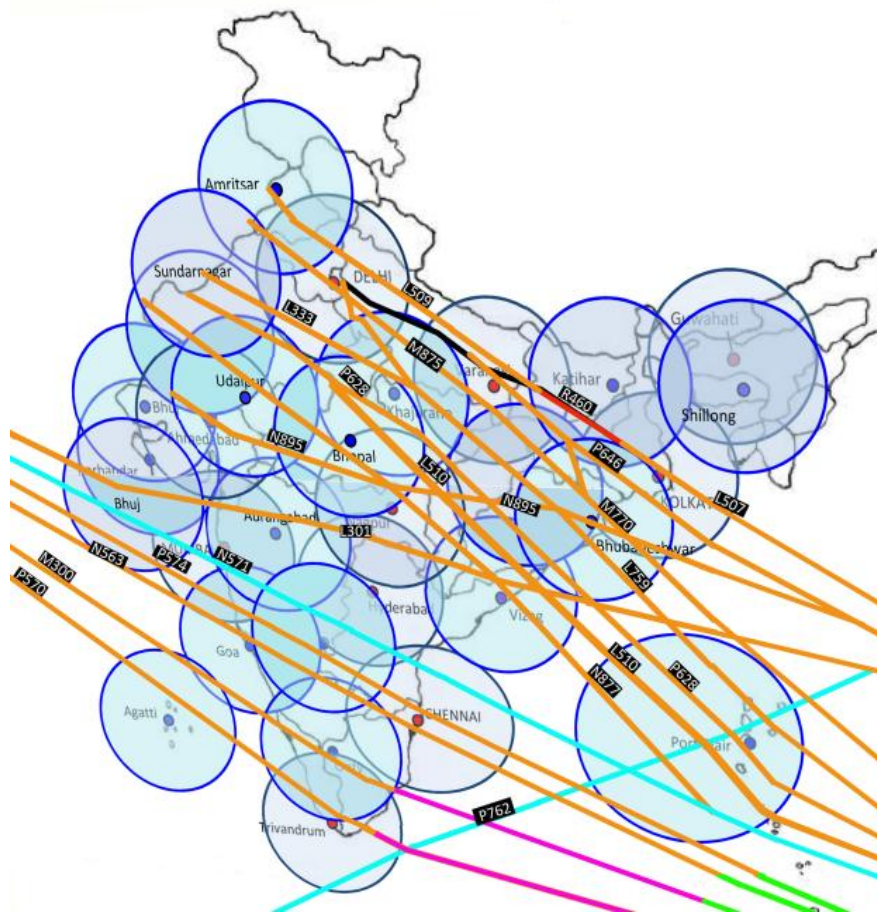


Figure3. VHF coverage map.

## 6. Analysis

The RNP10 routes in Bay of Bengal Arabian Sea airspace has been grouped into general traffic flows for analysis. The traffic flows are graphically depicted in Figure2.

Flow	Flow Description	RNP10 Routes
1.	Middle East to India, South East Asia and beyond.	P570, M300, N563, P574 & N571.
2.	Middle East to Bangkok and Far East.	L301.
3.	Europe to South East Asia.	N877, L510, P628, L759, M770, M875, N895, P646, L507, L509 & L333.
4.	South Africa and Sri Lanka to Bangkok and Far East.	P762.

Table3. Traffic Flows observed in the BOBASIO Airspace.

Table 3 lists the different flows. Figure4 illustrates the total traffic count and the number of over flights of each flow. Flow 1, Middle East to India, South East Asia and beyond Constitutes 42% of the total traffic.

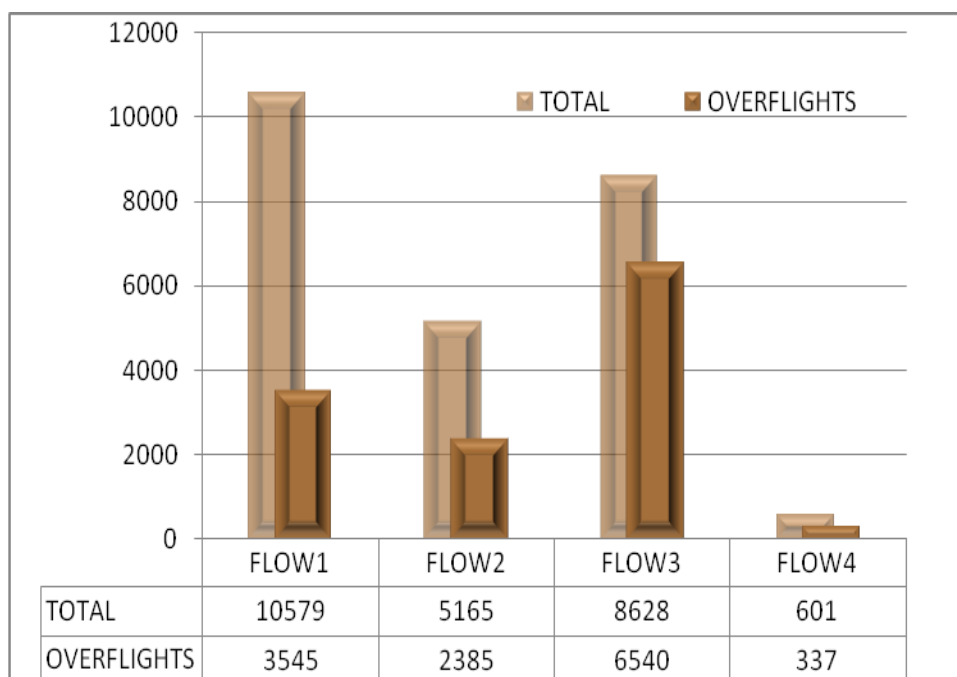


Figure4. Traffic count in each flow

6.1 Each Flow was analyzed in terms of Operators, Type of aircraft, Flight levels, and Peak traffic time. The time and Flight Level at the entry point into the Oceanic airspace was taken for determining the level usage and traffic density. The results of the analysis for the different Flows are detailed in the following sections.

6.2 **FLOW1 - Middle East to India, South East Asia and beyond.**

6.2.1 Traffic landing at, or departing from, Indian airports account for 67% of the traffic flow. N571 is the most utilized route with traffic to and from Indian destinations using this route. N563 is the least used route. A portion of N563 from LEKAP in the east to KAKIB in the west is not available from 0030UTC to 1630UTC.

6.2.2 About 60 Operators were found to be operating flights in this Flow. Figure 5 shows the top 20 operator wise distribution. The top 20 Operators represent 88% of the operations. Emirates airline operates the maximum number of flights, followed by Jet Airways. The Indian Airlines like Air India, Air India Express and Jet airways operate to and from Indian airports towards both middle East and South East Asia. The International operators operate flights to and from India as well as flights over flying India. Indian Operators account for 23% of the traffic flow.

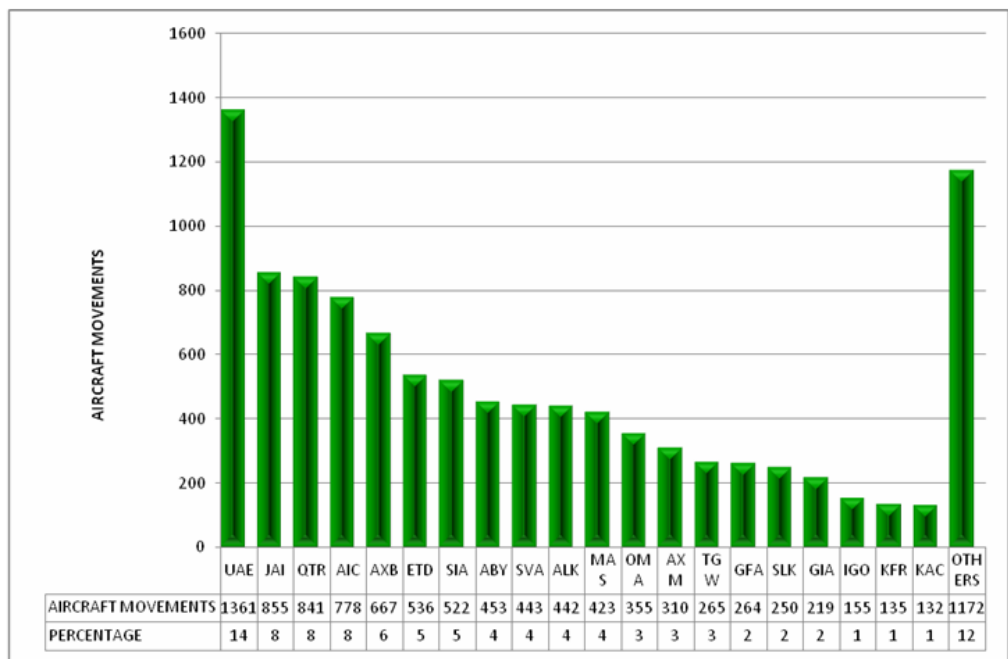


Figure5. Distribution of Operators in Flow1.

6.2.3 Figure 6 illustrates the top 15 aircraft types operated by the different airlines. A320 & B738 account for about 44% of the total movements which is mainly due to the traffic operating to and from India which lies in the middle of this Flow. There are 45 different type of aircraft of which the top 15 types account for 95% of the flight movements.

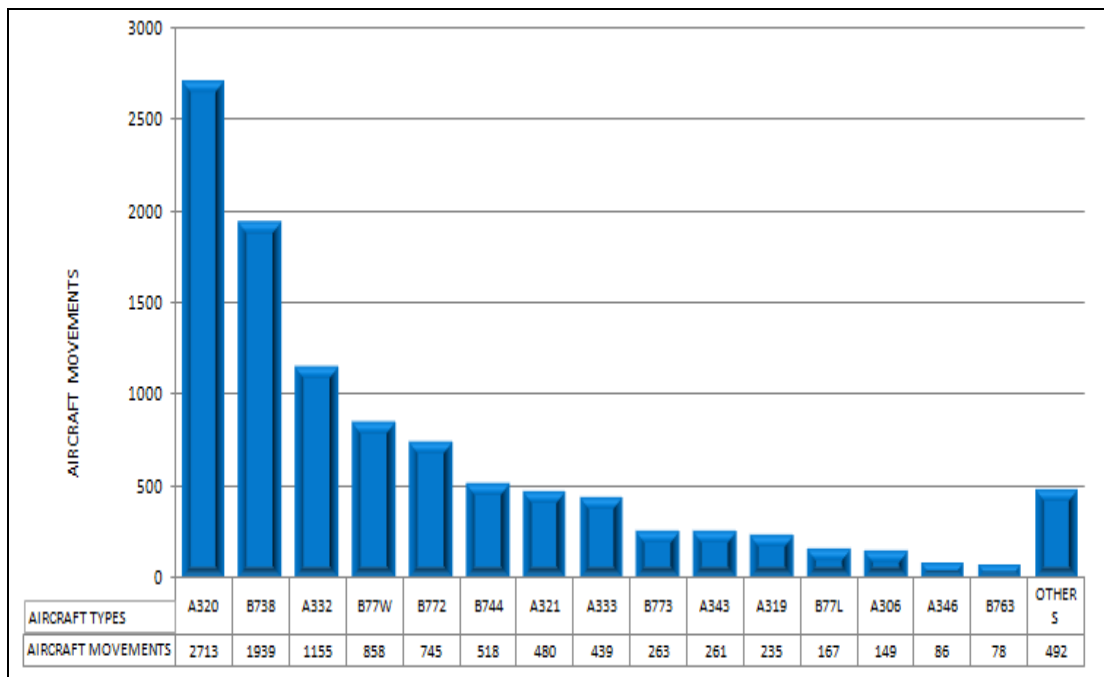


Figure6. Distribution of aircraft types in Flow1.

6.2.4 Figure 7 illustrates the Flight Level utilization. The most used westbound levels are FL360 & FL340 and east bounds FL570 & FL370. 85% of the flights had flown at FL340 and above.

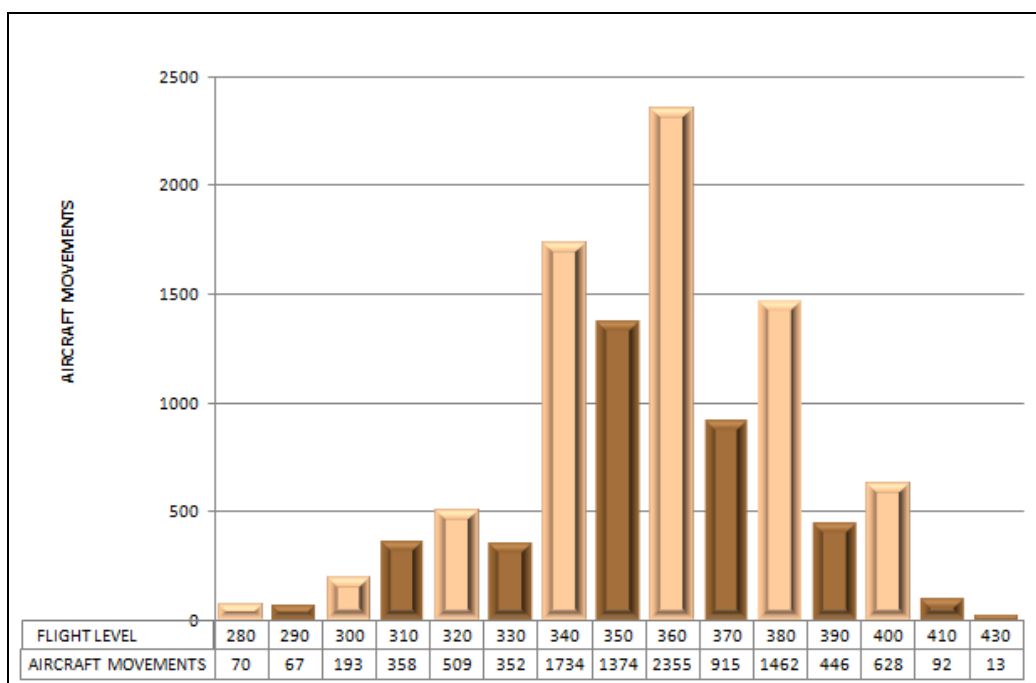


Figure7. Flight Level utilization in Flow1.

**6.3 Flow2 - Middle East to Bangkok and Far East.**

6.3.1 The traffic in this Flow is along a single route L301 which accounts for about 21% of the total traffic in all the four Flows. With a daily average of 166 aircraft movements L301 is the busiest route among the four Flows. It is also the most utilized RNP10 route used by international operators operating over flights across India. A segment of the route from BUSBO – AAU – NOBAT is not available from 0030UTC to 1300UTC. Aircraft operating outside these times should follow L505 between BUSBO to NOBAT. Restrictions are also imposed whenever Danger Area VED73 is active. Radar coverage is available along this route from NOBAT in the west to URKOK in the east.

6.3.2 The top 20 operators in this flow representing 86% of the movement is shown in Figure 8. The top 10 operators alone account for more than 70% of the traffic movements. Top operator Emirates had operated 936 movements during this period of which 458 were over flights across India.

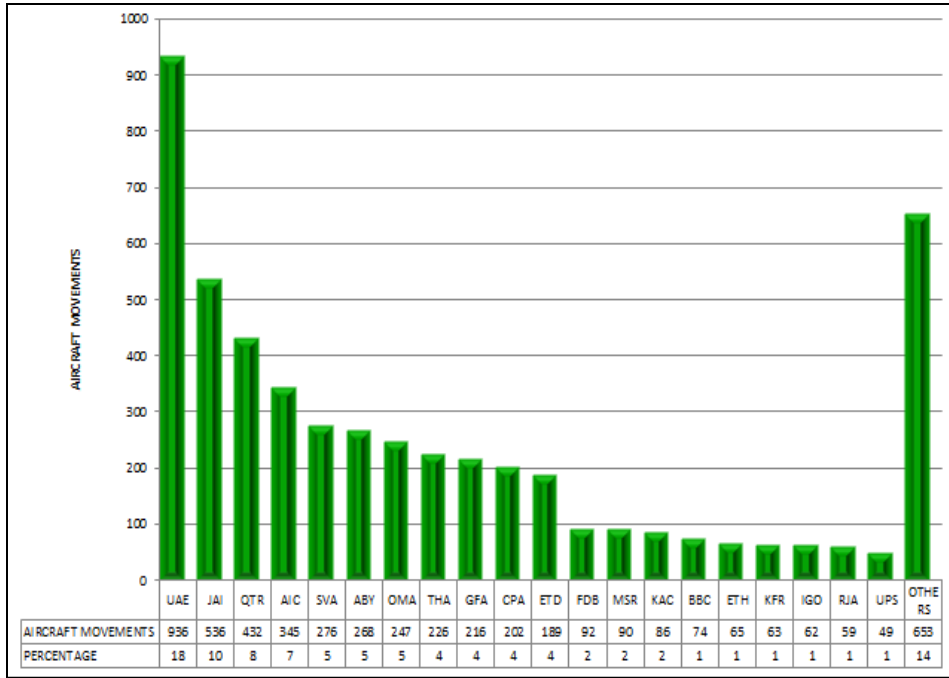


Figure8. Distribution of Operators in Flow2.

6.3.3 Figure9. Illustrates the top 15 aircraft types operating in this Flow. The top five aircraft types represent 62% of flight movements.

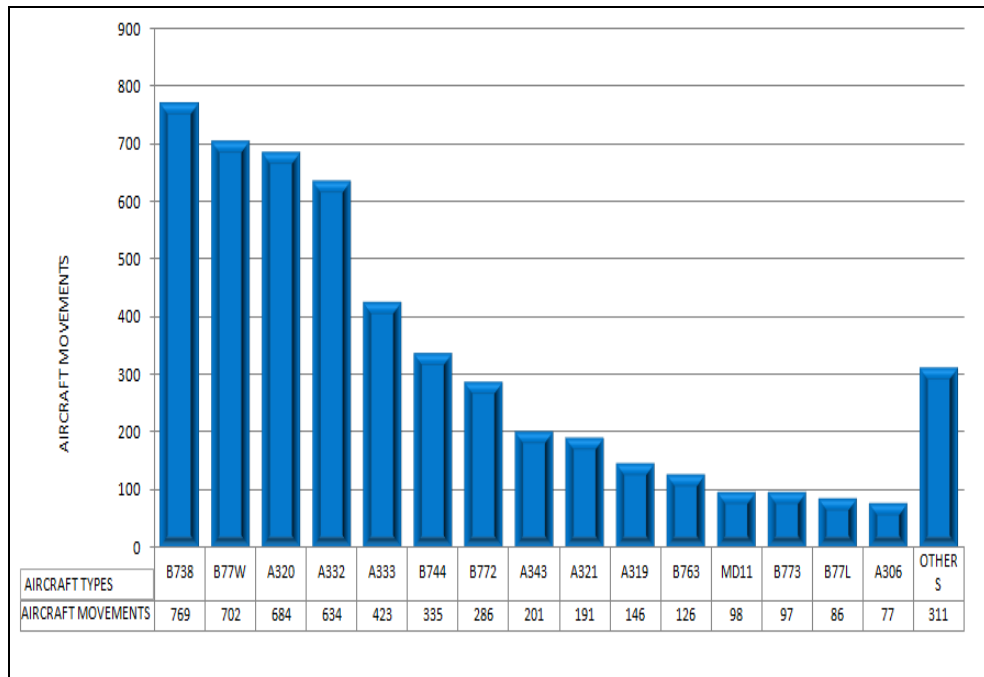


Figure9. Distribution of aircraft types in Flow2.

6.3.4 Figure 10. illustrates the Flight Level utilization. FL340, FL350, FL360 & FL370 are the most used Flight Levels with about 54% of the flights being accommodated at these levels.

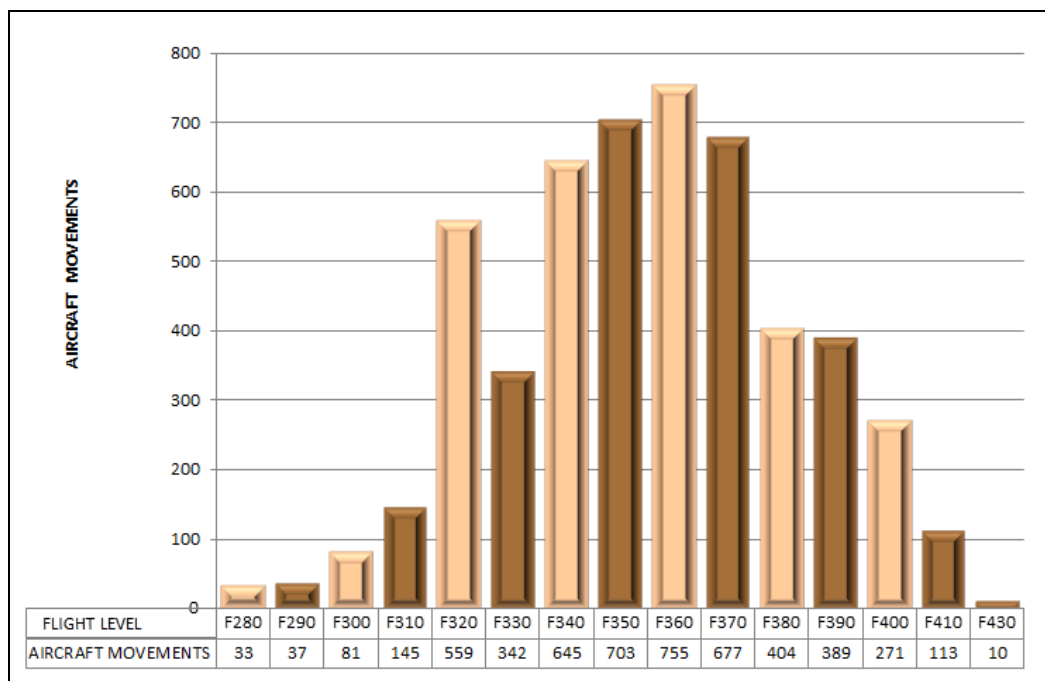


Figure10. Flight Level utilization in Flow2.

6.4 Flow 3 - Europe to South East Asia.

6.4.1 Traffic on this flow is along nine routes. About 76% of the traffic over-fly India.

6.4.2 Certain modifications in the route structure would help in seamless flow of traffic along these routes.

- Extending of N877 presently terminating at PRA in the west up to SERKA in Pakistan to join UL333 will help decongest P628 during peak traffic.
- Implementing RHS 50NM longitudinal on M875 & L333 will enable aircraft utilizing 50NM RLS on M770 & L759 to continue using the reduced separation up to GUGAL and TIGER respectively.
- Non RNP route R460 between CEA and GGC creates difficulty in implementing RHS on L507 and L509. However the MSSR radar at Varanasi is being used to ensure provision of seamless 50 NM RLS.

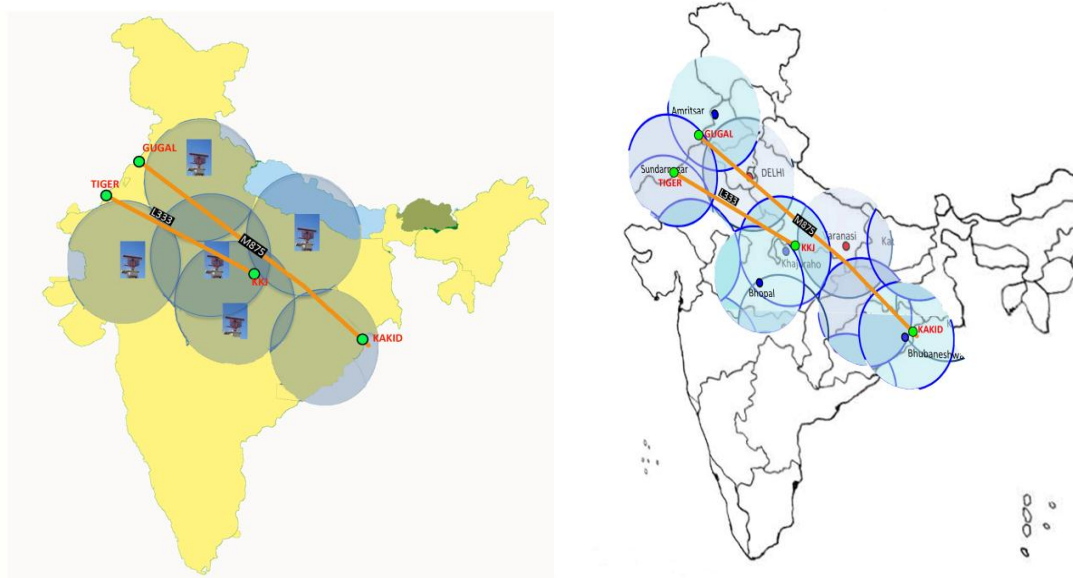


Figure11. Radar and VHF coverage on routes L333 & M875.

- 6.4.3 The eleven RNP10 routes in their transit across continental India cut across major Non – RNAV routes as well as high density domestic routes. However availability of seamless radar coverage and direct VHF communication helps resolve traffic conflicts and permit aircraft to be provided with 50NM reduced longitudinal separation.
- 6.4.4 The planned installation of ADS-B ground station at PPB will enable surveillance over the crucial airspace around Port Blair to resolve traffic conflicts over crossing points PPB, BIKEN, DOTEN, ALADO, SADAP, BASOP & LADER.
- 6.4.5 Figure 12 represents the top 20 operators using these routes. Top operator Thai airways accounts for 14% of the operations. Top eight operators operate 48% of the flight movements.

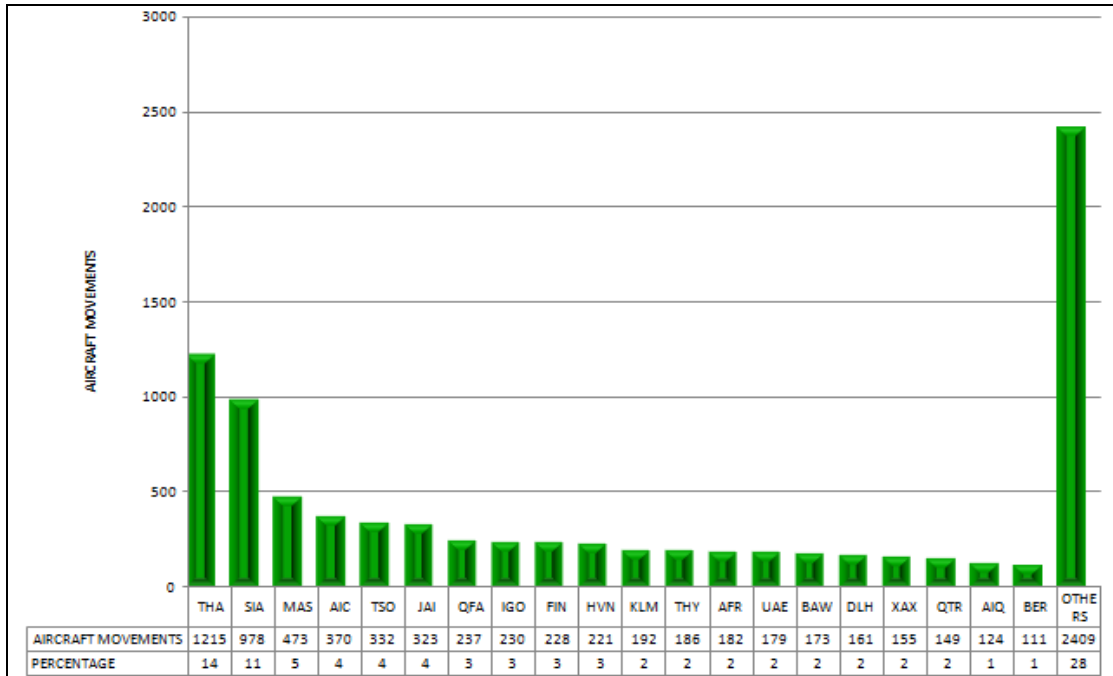


Figure 12. Distribution of aircraft Operators in Flow3.

- 6.4.6 The top fifteen aircraft types used is indicated in Figure 13. B744 is the top aircraft type used representing 16% of flight operations. The top 5 aircraft types represent 56% of flight movements.

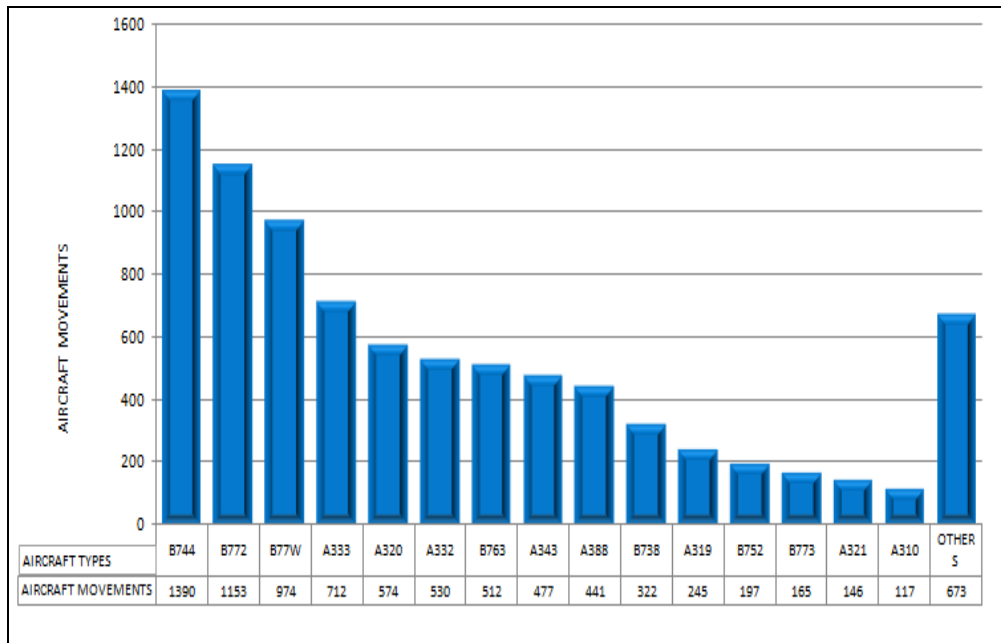


Figure13. Distribution of aircraft types in Flow3.

6.4.7 Figure 14 illustrates the Flight Level utilization. The most used Eastbound levels are FL370 & FL350. The most used Westbound levels are FL340 & FL300, this is due to the fact that only Flight Levels at the point of entry into the oceanic airspace had been considered.

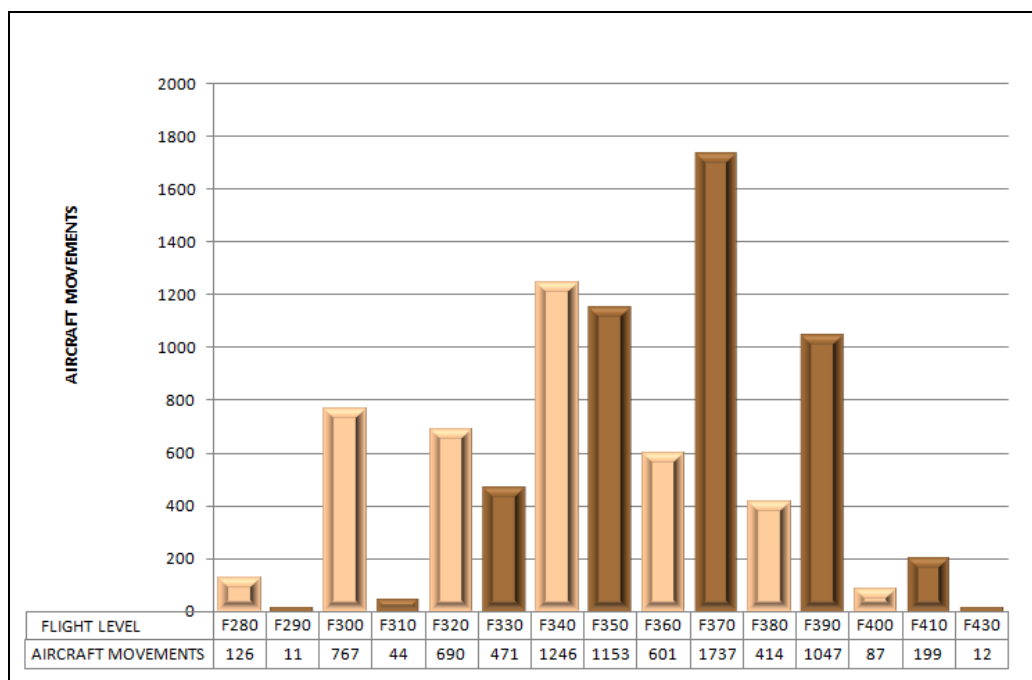


Figure14. Flight Level utilization in Flow3.

6.5 **Flow 4 - South Africa and Sri Lanka to South East Asia.**

6.5.1 Traffic flow is along P762 connecting Bangkok to Sri-Lanka. The route continues further downstream to South Africa as Non-RNAV route G465. Reduced Longitudinal Separation of 50NM was implemented on this route since 30<sup>th</sup> June 2011 but till date there was no opportunity to apply the reduced separation. Traffic to and from Indian airports operate on P761 which converges with P762 at PPB.

6.5.2 Figure 15. Shows the top ten operators along this route. The Top 3 operators alone account for 60% of flight operations.



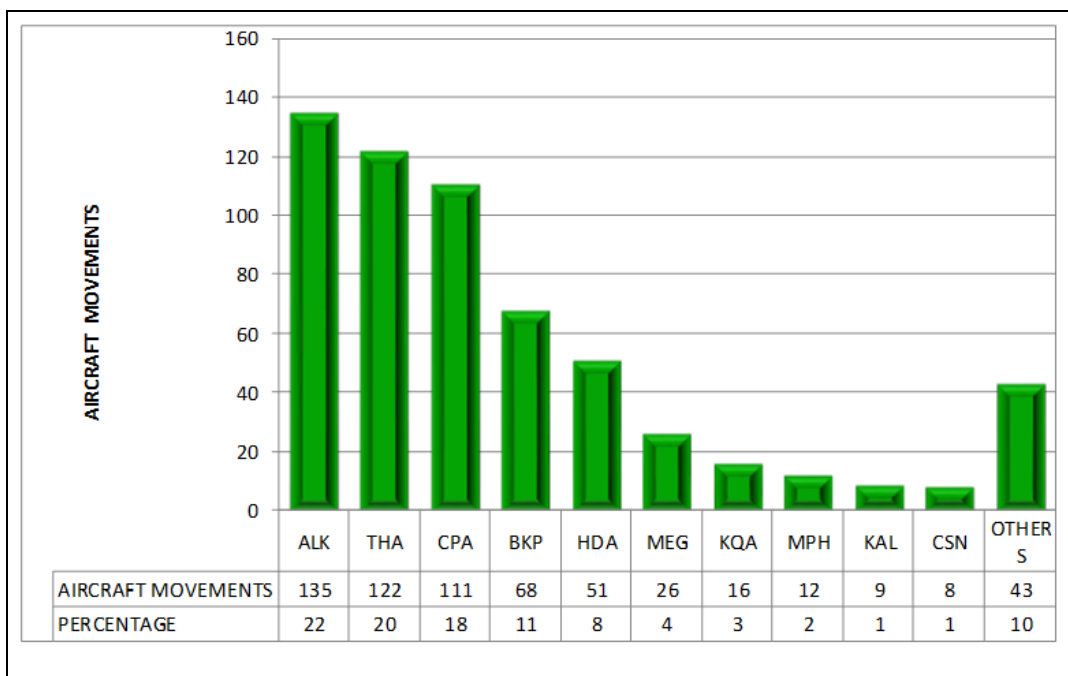


Figure15. Distribution of aircraft operators in Flow4.

6.5.3 Figure 16 shows the top 8 aircraft types used which account for 94% of flight movements.

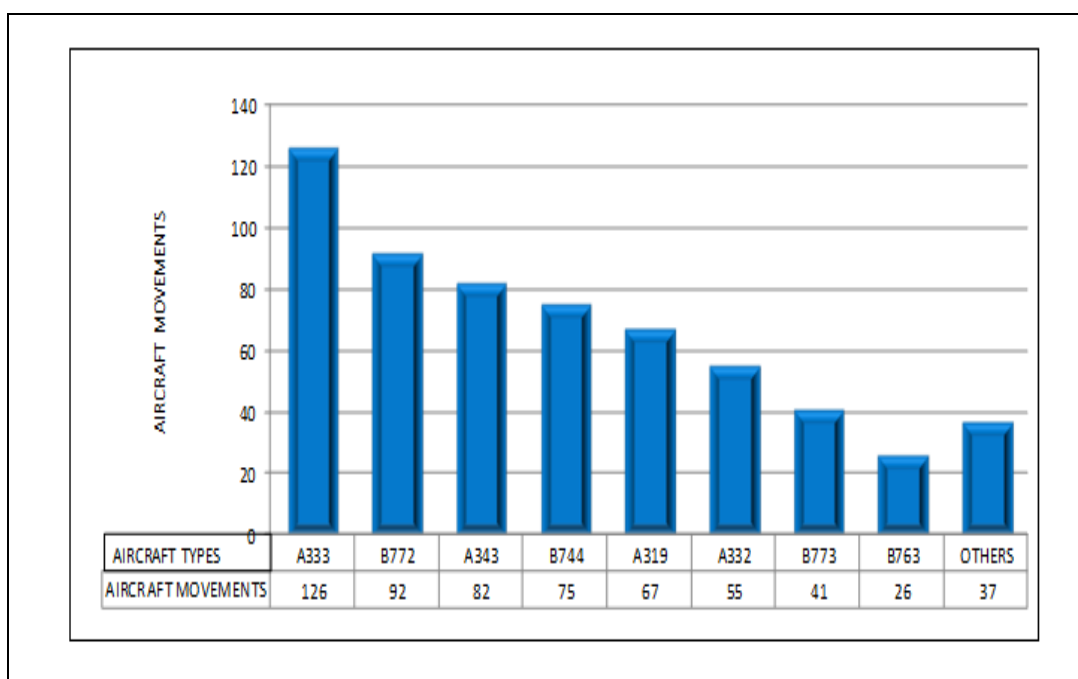


Figure16. Distribution of aircraft types in Flow4.

6.5.4 Figures 17 depict the Flight Level utilization. FL320 which is also the No PDC level on this route between Yangon and Chennai and FL360 are the most used westbound levels. FL360 & FL380 are mostly preferred by aircraft operating to African destinations. The most used Eastbound levels are FL310 & FL390.

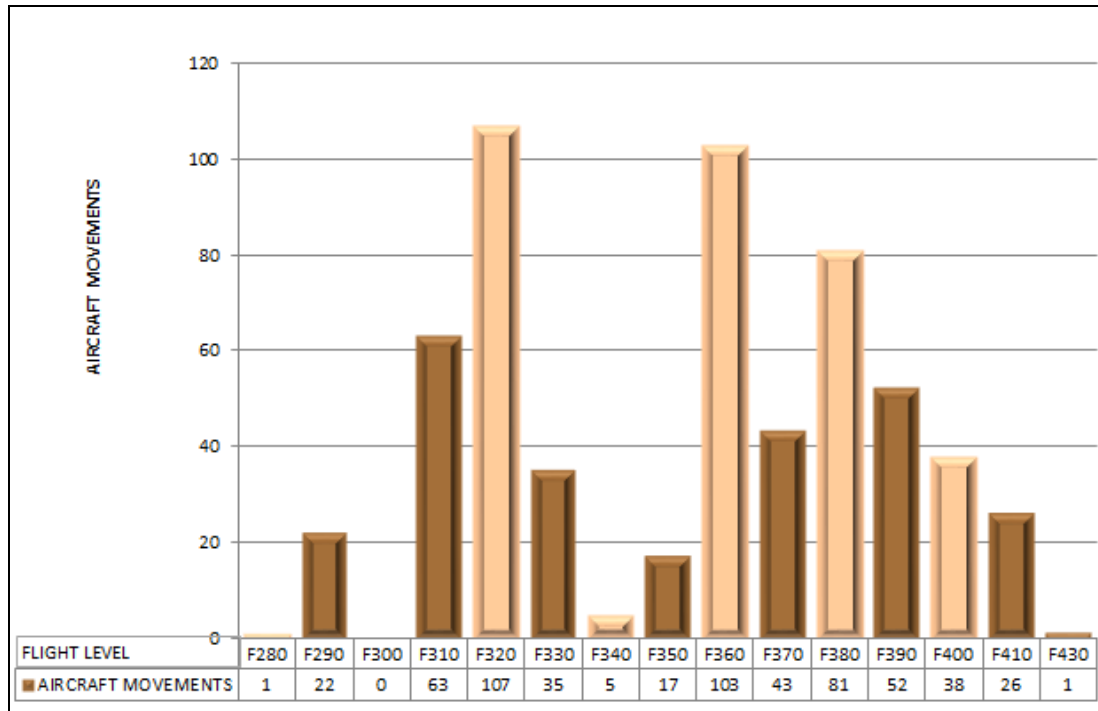


Figure17. Flight Level utilization in Flow4.

7. **Traffic Time Distribution**

The entry time was used to plot the traffic density on an hourly basis to determine the peak traffic periods for the four traffic flows. Figure 18 shows the traffic time distribution for the four flows.

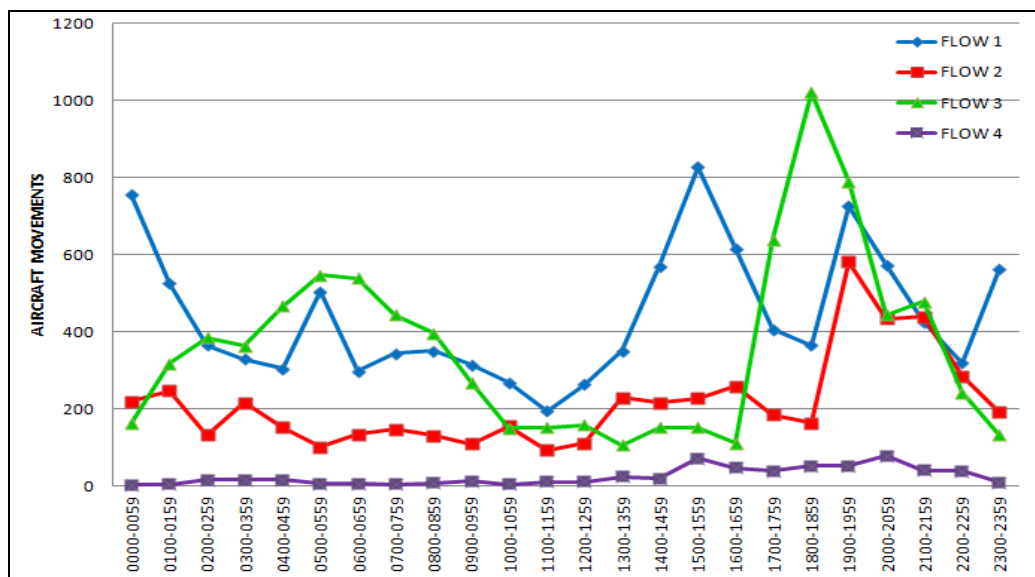


Figure18. Traffic Time Distribution.

## 8. Traffic between top City Pairs

The Traffic Sample Data was analyzed in terms of the departure and destination pairs to find the top city pairs among the four different flows. Figure 19 shows the Top 10 City Pairs which account for 17% of the total traffic.

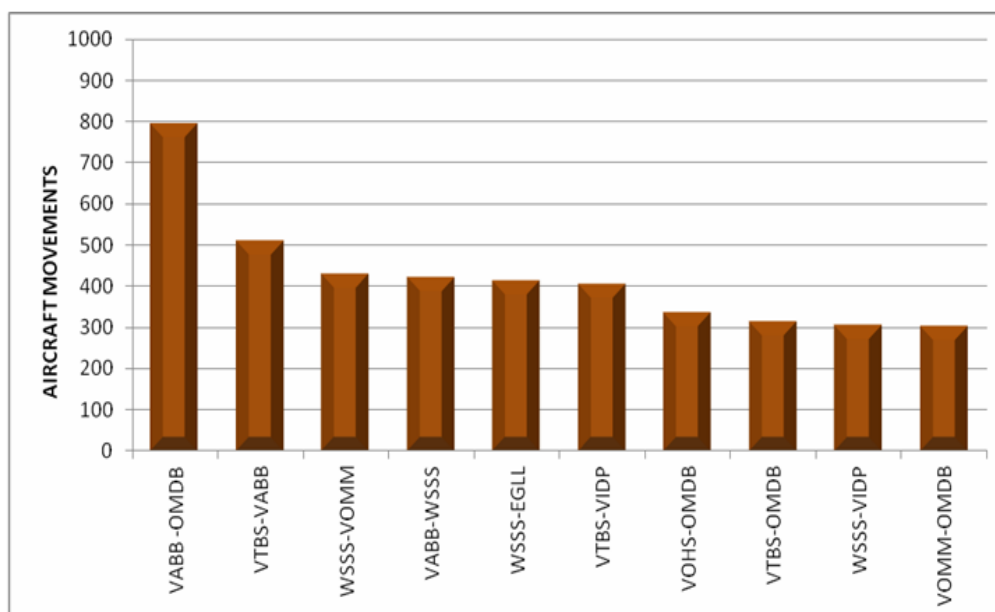


Figure19. Top ten City Pairs

## 9. 50NM RLS Post Implementation Analysis.

Data on the number of aircraft pairs provided with 50NM Reduced Longitudinal Separation was collected from 15th to 31st December 2011 from the three Indian ACCs. It has been observed from the data that non participation by other member states acts as an impediment in the implementation of RHS in the region.

- 9.1.1 Figure 20 shows the percentage of aircraft movements provided with 50NM RLS during the period with in Chennai FIR. There were only two instances when 50 NM RLS was used between two aircraft by Chennai controllers. There was initial confusion between controllers in Chennai and Kualalumpur over implementation on N571, P628 & L510 which was sorted out immediately. Though Kualalumpur was ready to accept eastbound aircraft pairs with 50 NM RLS there were no instance of westbound flights with 50 NM RLS entering Chennai FIR. Further with Colombo set to join the implementation only in Phase 2C, from 8<sup>th</sup> March 2012 and P762 on which 50 NM RLS was implemented in Phase1 being a low density traffic route witnessing no instance of use of 50 NM RLS till date, the benefit of implementation of 50 NM RLS has so far been minimal.

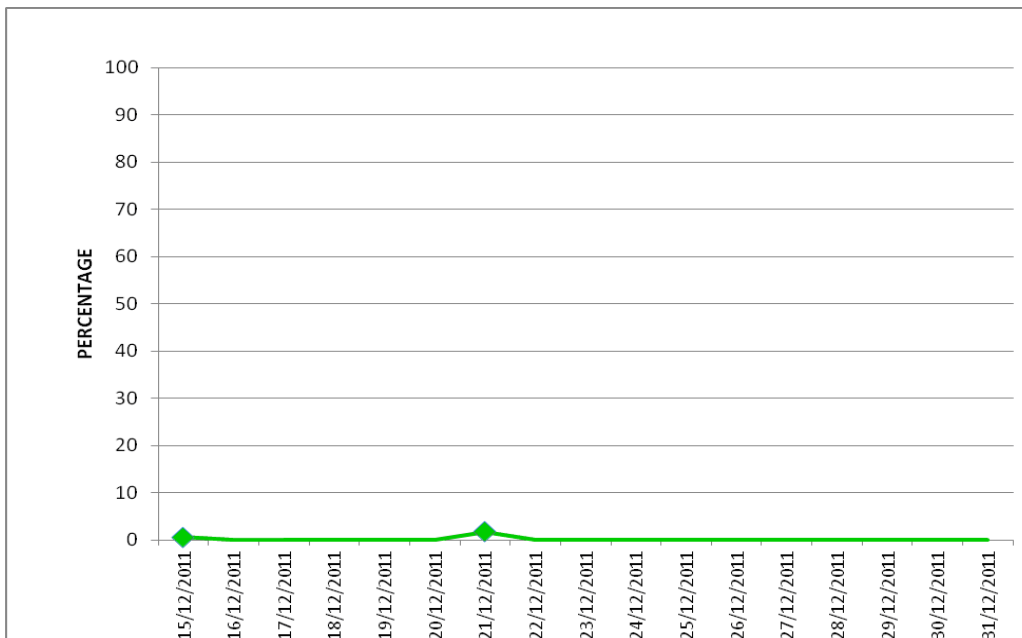


Figure20: Percentage of aircraft operations with 50NM RLS in Chennai FIR

9.1.2 Figure 21 shows the percentage of aircraft movements provided with 50 NM RLS within Mumbai FIR. Since Muscat had expressed their inability to implement 50NM RLS Mumbai ACC has to restrict the use of 50NM RLS by westbound flights in the Arabian Sea. Westbound aircraft pairs with 50NM RLS, needs to be provided with alternate forms of separation before it is released to Muscat ACC on routes. Factors such as high traffic density, crossing routes, limited VHF coverage and data link capability of aircraft affect the ability of the controller to effect alternate forms of separation between such aircraft prior to releasing to Muscat ACC. As radar coverage within Muscat FIR extends up to the boundary with Mumbai FIR, implementation of 50 NM RLS is only beneficial for Muscat as they need to expand the longitudinal separation between suitably equipped east bound aircraft pairs from 10 NM to only 50 and westbound flights with 50 NM RLS, exiting Mumbai FIR will be within the radar coverage of Muscat. This will ensure a seamless flow of aircraft pairs with 50NM RLS.

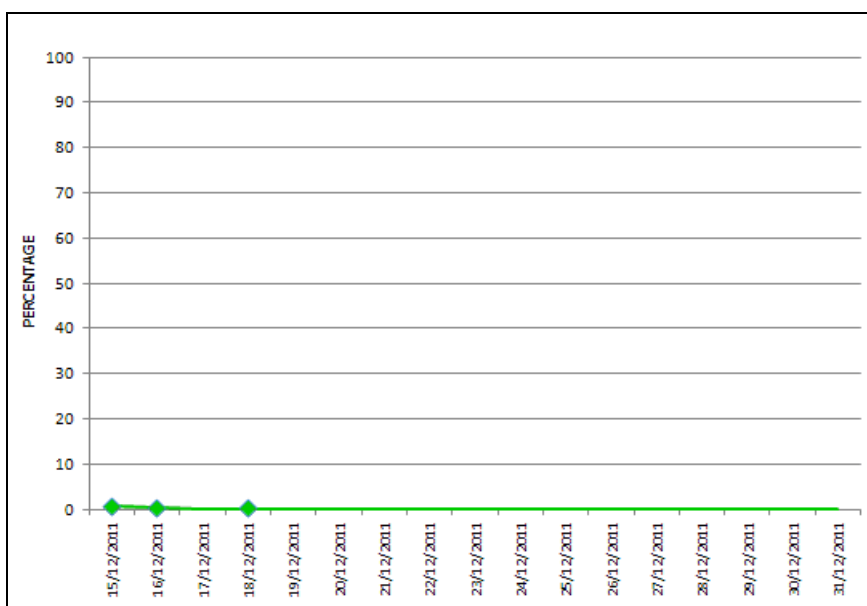


Figure 21: Percentage of aircraft operations with 50 NM RLS in Mumbai FIR

- 9.1.3 Figure 22 shows the percentage of aircraft pairs with 50 NM RLS observed in Kolkata FIR. Sixty percent of the aircraft pair provided with 50 NM RLS were logged on data link and forty percent on VHF voice communication.

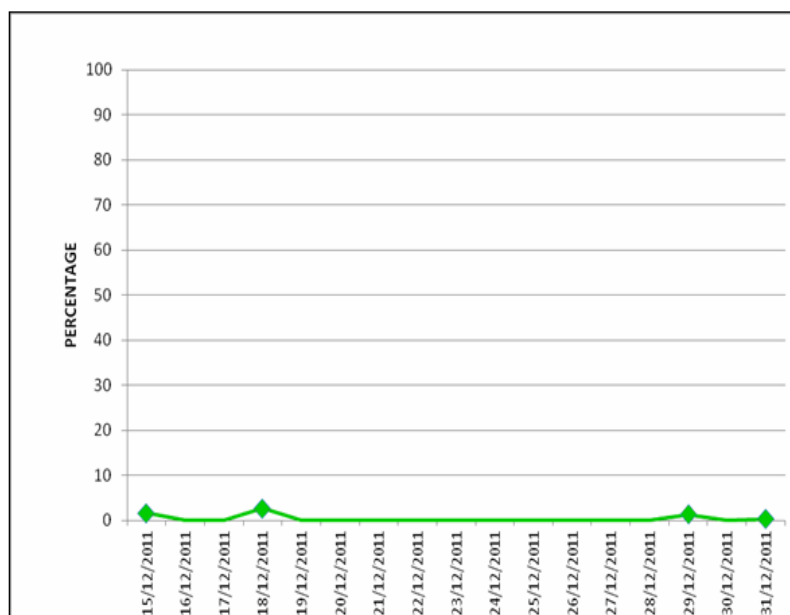


Figure22: Percentage of aircraft operations with 50 NM RLS in Kolkata FIR

## 10. Conclusion

It can be concluded that, presence of Non-RNP10 routes, either between two RNP10 routes or as an extension of an RNP10 route affects the seamless implementation of 50 NM RLS. The proposed implementation of 50NM RLS on M875 & L333 by India and realigning the route from PRA to Nawabshar in Karachi FIR and then on to SERKA to a more direct route will enhance seamless flow of traffic using 50NM Reduced longitudinal Separation across the continental airspace of India, Pakistan and Afghanistan. Also an increase in the percentage of aircraft with data link capability will enhance the confidence of controllers in implementing reduced longitudinal separation. Further participation by Muscat ACC would benefit operators using the east west corridor connecting South East Asia with Middle East.

**Lateral and Longitudinal Collision Risk Assessment****of****Bay of Bengal , Arabian Sea and Indian Ocean Airspace region****1. Introduction**

In this article we reinvestigate the collision risk between two aircraft flying over the Bay of Bengal, Arabian Sea, and Indian Ocean (BOBASIO) region. This safety assessment is undertaken jointly by the Airports Authority of India (AAI) and the Indian Statistical Institute, Delhi Centre under the MoA signed between the two organizations on January 13, 2011. The goal of this study is to confirm that the Target Level of Safety (TLS) which is  $5 \times 10^{-9}$  fatal accidents per flight hour, is currently met.

Note that in the following routes in the BOBASIO region reduced horizontal separation (RHS) was introduced in two phases:

- Phase 1: On the routes N571 and P762 from July 2011 and
- Phase 2: On the routes L301, L507, L509, L510, L759, M300, M770, N563, N877, N895, P570, P574, P628 and P646 from December 15, 2011.

Thus currently the separation standards are as follows

- for lateral separation it is at least 50 NM between all the parallel routes;
- for longitudinal it is at least 10 minutes leading to an average 80 NM between front and behind aircraft on all routes except those mentioned above where the separation standard is reduced to 50 NM between front and behind aircraft.

In this article we carry out the quantitative risk analysis based on two types of datasets supplied by the AAI.

- **Traffic Sample Data (TSD):**

Traffic sample data from Chennai, Kolkata, Mumbai, and Colombo FIRs for the month of December 2011 was used. The original data contained several anomalies, which we tried to detect and remove. Briefly, the following initial filtering criteria were used:

- Any duplication was removed.
- Records with Exit time less than Entry time were removed.
- Records with flight level less than F290 were removed.

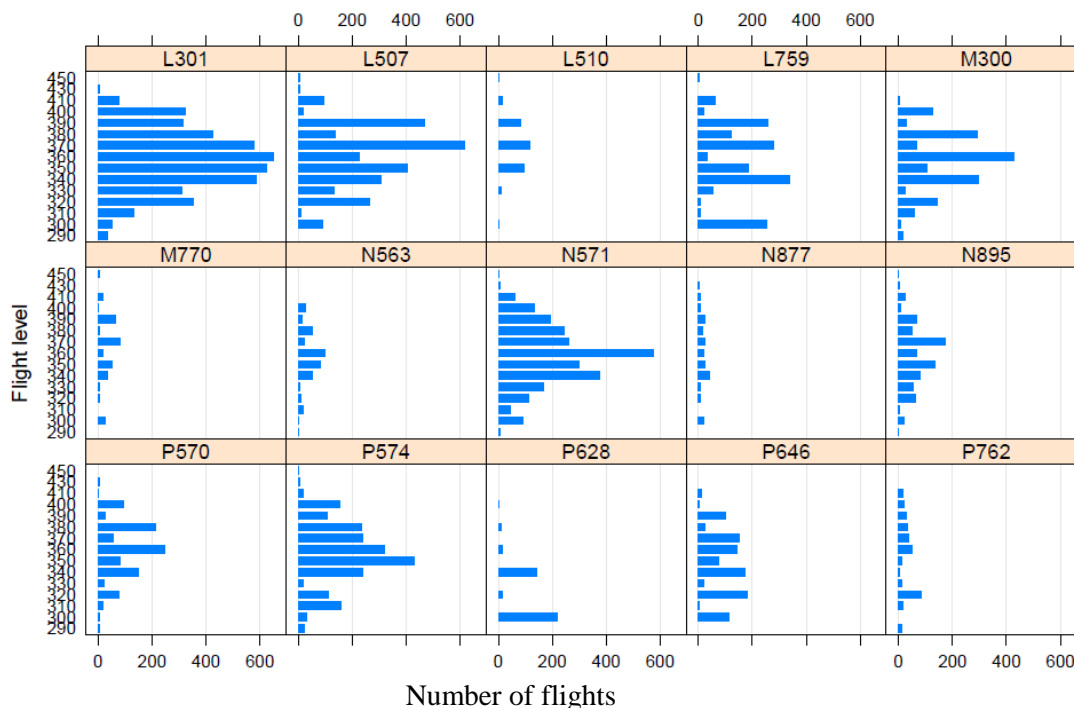


Figure 1: Number of flights by route and flight level in Chennai, Kolkata, Mumbai and Colombo FIRs, based on December 2011 TSD. Only RHS routes are shown.

31857 records that were retained after filtering were considered for the subsequent statistical analysis. Figure 1 provides a graphical summary of the number of flights by route and flight level for RHS routes.

- **Gross Navigational Error (GNE) Data:**

Reports of Gross Navigational Errors were received from India (Chennai, Kolkata, Mangalore and Mumbai FIRs), Bangkok, Malaysia and Yangon as summarized in Table 1.

Year	Month	FIR	Flights	LLE	LLD
2010	AUGUST	KOLKATA	443	0.00	0.00
2010	SEPTEMBER	KOLKATA	423	0.00	0.00
2010	OCTOBER	KOLKATA	432	0.00	0.00
2010	NOVEMBER	KOLKATA	427	0.00	0.00
2010	DECEMBER	KOLKATA	545	0.00	0.00
2010	JULY	CHENNAI	2679	0.00	0.00
2010	AUGUST	CHENNAI	5173	0.00	0.00
2010	SEPTEMBER	CHENNAI	5196	0.00	0.00
2010	OCTOBER	CHENNAI	5478	0.00	0.00
2010	NOVEMBER	CHENNAI	5258	0.00	0.00
2010	DECEMBER	CHENNAI	5432	0.00	0.00
2010	JULY	MUMBAI	1838	0.00	0.00
2010	AUGUST	MUMBAI	1812	0.00	0.00
2010	SEPTEMBER	MUMBAI	1792	0.00	0.00
2010	OCTOBER	MUMBAI	1884	0.00	0.00
2010	NOVEMBER	MUMBAI	1068	0.00	0.00
2010	DECEMBER	MUMBAI	1426	0.00	0.00

2010	JULY	BANGKOK	1865	0.00	0.00
2010	AUGUST	BANGKOK	2330	0.00	0.00
2010	SEPTEMBER	BANGKOK	2297	0.00	0.00
2010	OCTOBER	BANGKOK	2234	0.00	0.00
2010	NOVEMBER	BANGKOK	2108	0.00	0.00
2010	DECEMBER	BANGKOK	2061	0.00	0.00
2010	JULY	MALAYSIA	2693	0.00	0.00
2010	AUGUST	MALAYSIA	2734	0.00	0.00
2010	SEPTEMBER	MALAYSIA	2702	0.00	0.00
2010	OCTOBER	MALAYSIA	2778	0.00	0.00
2010	NOVEMBER	MALAYSIA	2433	0.00	0.00
2010	DECEMBER	MALAYSIA	2401	0.00	0.00
2010	SEPTEMBER	YANGON	563	0.00	0.00
2010	OCTOBER	YANGON	600	0.00	0.00
2010	NOVEMBER	YANGON	578	0.00	0.00
2010	DECEMBER	YANGON	597	0.00	0.00
2011	JANUARY	KOLKATA	690	0.00	0.00
2011	FEBRUARY	KOLKATA	680	0.00	0.00
2011	MARCH	KOLKATA	729	0.00	0.00
2011	APRIL	KOLKATA	851	0.00	0.00
2011	MAY	KOLKATA	2001	0.00	0.00
2011	JANUARY	CHENNAI	1812	0.00	0.00
2011	FEBRUARY	CHENNAI	1640	0.00	0.00
2011	MARCH	CHENNAI	1899	0.00	0.00
2011	APRIL	CHENNAI	1734	0.00	0.00
2011	MAY	CHENNAI	1934	0.00	0.00
2011	JANUARY	MUMBAI	1488	0.00	0.00
2011	FEBRUARY	MUMBAI	1384	0.00	0.00
2011	MARCH	MUMBAI	1458	0.00	0.00
2011	APRIL	MUMBAI	1458	0.00	0.00
2011	MAY	MUMBAI	1302	0.00	0.00
2011	JANUARY	MALAYSIA	2356	0.00	0.00
2011	FEBRUARY	MALAYSIA	2246	0.00	0.00
2011	MARCH	MALAYSIA	2434	0.00	0.00
2011	APRIL	MALAYSIA	2612	0.00	0.00
2011	JANUARY	YANGON	5200	0.00	0.00
2011	FEBRUARY	YANGON	4566	0.00	0.00
2011	MARCH	YANGON	5242	0.00	0.00
2011	APRIL	YANGON	4682	0.00	0.00
2011	MAY	YANGON	5573	0.00	0.00
2011	JUNE	KOLKATA	1820	0.00	0.00
2011	JULY	KOLKATA	1919	0.00	0.00
2011	AUGUST	KOLKATA	1868	0.00	0.00
2011	SEPTEMBER	KOLKATA	1765	0.00	0.00
2011	OCTOBER	KOLKATA	2082	0.00	0.00
2011	NOVEMBER	KOLKATA	2113	0.00	0.00
2011	DECEMBER	KOLKATA	2318	0.00	0.00



2011	JUNE	CHENNAI	1818	0.00	0.00
2011	JULY	CHENNAI	1963	0.00	0.00
2011	AUGUST	CHENNAI	2019	0.00	0.00
2011	SEPTEMBER	CHENNAI	1872	0.00	0.00
2011	OCTOBER	CHENNAI	1957	0.00	0.00
2011	NOVEMBER	CHENNAI	1848	0.00	0.00
2011	DECEMBER	CHENNAI	5026	0.00	0.00
2011	JUNE	MUMBAI	9436	0.00	0.00
2011	JULY	MUMBAI	8283	0.00	0.00
2011	AUGUST	MUMBAI	11019	0.00	0.00
2011	SEPTEMBER	MUMBAI	11616	0.00	0.00
2011	OCTOBER	MUMBAI	12659	0.00	0.00
2011	NOVEMBER	MUMBAI	12869	0.00	0.00
2011	DECEMBER	MUMBAI	12276	0.00	0.00
2011	MAY	BANGKOK	1807	0.00	0.00
2011	JUNE	BANGKOK	4800	0.00	0.00
2011	JULY	BANGKOK	5309	0.00	0.00
2011	AUGUST	BANGKOK	5365	0.00	0.00
2011	SEPTEMBER	BANGKOK	4847	0.00	0.00
2011	OCTOBER	BANGKOK	5907	0.00	0.00
2011	NOVEMBER	BANGKOK	6680	0.00	0.00
2011	DECEMBER	BANGKOK	6752	0.00	0.00
2011	MAY	MALAYSIA	2614	0.00	0.00
2011	JUNE	MALAYSIA	2580	0.00	0.00
2011	JULY	MALAYSIA	2710	0.00	0.00
2011	AUGUST	MALAYSIA	2518	0.00	0.00
2011	SEPTEMBER	MALAYSIA	2735	0.00	0.00
2011	OCTOBER	MALAYSIA	2922	0.00	0.00
2011	NOVEMBER	MALAYSIA	2780	0.00	0.00
2011	DECEMBER	MALAYSIA	2411	0.00	0.00
2011	JUNE	YANGON	4560	0.00	0.00
2011	JULY	YANGON	5060	0.00	0.00
2011	AUGUST	YANGON	4778	0.00	0.00
2011	SEPTEMBER	YANGON	9381	0.00	0.00
2011	NOVEMBER	YANGON	9665	0.00	0.00
2011	MAY	MANGALORE	3894	0.00	0.00
2011	JUNE	MANGALORE	3861	0.00	0.00
2011	JULY	MANGALORE	4089	0.00	0.00
2011	AUGUST	MANGALORE	3983	0.00	0.00
2011	SEPTEMBER	MANGALORE	3786	0.00	0.00
2011	OCTOBER	MANGALORE	3584	0.00	0.00
2011	NOVEMBER	MANGALORE	3309	0.00	0.00
2011	DECEMBER	MANGALORE	3644	0.00	0.00
Total			363128	0.00	0.00

Table 1: Summary of reports of Gross Navigational Errors.

In Section 2 we discuss the risk assessment for the lateral direction and Section 3 gives the same for the longitudinal direction.

## 2. Lateral Collision Risk Assessment

### 2.1 Lateral Collision Risk Model

In order to compute the level of safety for lateral deviations of operations on the BOBASIO region we use the Reich Lateral Collision Risk Model. It models the lateral collision risk due to the loss of lateral separation between aircraft on adjacent parallel tracks flying at the same flight level. The model is as follows:

$$N_{ay} = P_y(S_y) P_z(0) \frac{\lambda_x}{S_x} \left\{ E_y(\text{same}) \left[ \frac{|\Delta V|}{2\lambda_x} + \frac{|\dot{y}(S_y)|}{2\lambda_y} + \frac{|\dot{z}|}{2\lambda_z} \right] + E_y(\text{opp}) \left[ \frac{2|V|}{2\lambda_x} + \frac{|\dot{y}(S_y)|}{2\lambda_y} + \frac{|\dot{z}|}{2\lambda_z} \right] \right\} \quad (1)$$

We would like to note that same model has been used for the safety assessment study of the South China Sea which was carried out by SEASMA and also in European safety assessment which was carried out for EUR/SAM corridor.

The parameters in the equation (1) are defined as follows:

- $N_{ay}$  := Expected number of fatal accidents (two for every collision) per flight hour due to the loss of lateral separation between co-altitude aircraft flying on tracks with planned  $S_y$  NM lateral separation.
- $S_y$  := Minimum planned lateral separation.
- $\lambda_x$  := Average length of an aircraft flying in BOBASIO region..
- $\lambda_y$  := Average wingspan of an aircraft flying in BOBASIO region..
- $\lambda_z$  := Average height of an aircraft flying in BOBASIO region..
- $P_y(S_y)$  := Probability of lateral overlap of aircraft nominally flying on adjacent flight paths, separated by  $S_y$  NM.
- $P_z(0)$  := Probability of vertical overlap of aircraft assigned to same flight path at the same flight level.
- $S_x$  := Length of half the interval in NM used to count proximate aircraft at adjacent routes.
- $E_y(\text{same})$  := Same direction lateral occupancy at same assigned flight level.
- $E_y(\text{opp})$  := Opposite direction lateral occupancy at same assigned flight level.
- $|\Delta V|$  := Average relative speed of two aircraft flying on parallel routes in same direction.
- $|V|$  := Average ground speed on an aircraft.
- $|\dot{y}(S_y)|$  := Average relative lateral speed of aircraft pair at loss of planned lateral separation of  $S_y$ .
- $|\dot{z}|$  := Average relative vertical speed of a co-altitude aircraft pair assigned to the same route.

A collision and consequently two fatal accidents, can only occur if there is overlap between two aircraft in all three dimensions simultaneously. Equation (1) gathers the product of the probabilities of losing separation in each one of the three dimensions. As it has already been said,  $P_z(0)$  is the probability of vertical overlap;  $P_y(S_y)$  is the probability of lateral overlap and the combinations of  $\frac{\lambda_x}{S_x} E_y(\text{same})$  and  $\frac{\lambda_x}{S_x} E_y(\text{opp})$  relate to the probability of longitudinal overlap of aircraft on adjacent parallel tracks and at the same flight level. All the probabilities can be interpreted as proportions of flight time in the airspace during which overlap in the pertinent dimension occurs. As the collision risk is expressed as the expected number of fatal accidents per flight hour, the joint overlap probability must be converted into number of events involving joint overlap in the three dimensions, relating overlap probability with *passing frequency*. Here we note that passing frequency between two adjacent routes is the average number of events, per flight hour, in which two aircraft are in longitudinal overlap when travelling in the opposite or same direction at the same flight level. This is achieved by

means of the expressions  $\frac{|\Delta V|}{2V}$  within square brackets in Equation (1). Each of the terms within square brackets represents the reciprocal of the average duration of an overlap in one of the dimensions. For example, is the reciprocal of the average duration of an overlap  $\frac{2|V|}{2\lambda_x}$  in the longitudinal direction for same direction traffic. In the case of longitudinal direction too, but for opposite direction, the average relative speed is  $2V$  and the average overlap time is

The model is based on the following hypothesis:

- All routes are parallel.<sup>1</sup>
- All collisions normally occur between aircraft on adjacent routes, although, if the probability of overlap is significantly large, they may also occur on non-adjacent routes.
- The entry times into the track system are statistically independent.
- The lateral deviations of aircraft on adjacent tracks are statistically independent.
- The vertical, longitudinal and lateral deviations of an aircraft are statistically independent.
- The aircraft are replaced by rectangular boxes.
- There is no corrective action by pilots or ATC when two aircraft are about to collide.

The model also assumes that the nature of the events making up the lateral collision risk is completely random. This implies that any location within the system can be used to collect a representative data sample on the performance of the system.

## 2.2 Estimated Values of the Parameters and Estimated Lateral Collision Risk

The following table gives the values of the parameters of the right-hand side of the equation (1) which are obtained from our analysis.

Parameter	Estimated Values	Source of the Estimate
$S_y$	50 NM	Current minimum lateral separation.
$\lambda_x$	0.04065875 NM	Estimated from TSD (see Section 2.3).
$\lambda_y$	0.04308855 NM	Estimated from TSD (see Section 2.3).
$\lambda_z$	0.01301296 NM	Estimated from TSD (see Section 2.3).
$P_y(50)$	$3.67207 \times 10^{-8}$	Estimated using a mixture model (see Section 2.4).
$P_z(0)$	0.538	Conservative value used in previous safety assessments (see Section 2.5).
$S_x$	80 NM	Equivalent to $\pm 10$ -minutes of longitudinal separation.
$E_y(\text{same})$	0.08951841	Estimated from the TSD (see Section 2.6).
$E_y(\text{opp})$	0	No opposite directional lateral occupancy at same assigned flight level.
$ \Delta V $	19 knots	Value obtained from TSD (see Section 2.8).
$ \dot{y}(50) $	75 knots	Conservative value taken from EMA Handbook (see Section 2.9).
$ \dot{z} $	1.5 knots	Conservative value as per EMA Handbook (see Section 2.10).

Finally this leads to the following estimate for the lateral collision risk  $N_{ay}$ .

$$N_{ay} = 1.04405 \times 10^{-9}$$

<sup>1</sup> In the BOBASIO region there are cross route, such as, P762. A stricter time separation is imposed on such a route but we ignore that to be more conservative about our estimates.

### 2.3 Estimating Average Aircraft Dimensions

Table 2 summarizes the distribution of aircraft population in the TSD. To be conservative, we used the maximum aircraft dimensions.

	Length	Wingspan	Height	Flights
A320	37.57	34.10	11.76	3681
B77W	73.90	64.80	18.50	2945
B738	39.20	34.40	12.57	2926
A332	58.80	60.30	17.40	2555
B744	70.60	64.80	19.40	2008
B772	63.70	60.90	18.40	1960
A333	63.60	60.30	16.85	1714
A343	63.60	60.30	16.85	1040
A321	44.51	34.10	11.76	776
B763	54.90	47.60	15.90	628
B773	73.90	60.90	18.40	589
A388	73.00	79.80	24.10	527
A319	33.84	34.10	11.76	504
B77L	63.70	64.80	18.30	413
A346	75.30	63.45	17.30	239
A306	54.10	44.84	16.54	222
A310	46.66	43.90	15.80	179
MD11	61.20	51.70	17.60	160
B752	47.30	38.10	13.60	155
A345	67.90	63.45	17.10	106
B743	70.60	59.60	19.30	96
B74S	56.30	59.60	20.00	43
CL60	20.85	19.60	6.30	33
B737	33.60	34.30	12.60	32
GLF4	26.90	23.70	7.40	31
GLEX	30.30	26.90	7.60	29
F2TH	20.20	19.30	7.10	21
B742	70.60	59.60	19.30	21
H25B	15.60	15.70	5.40	15
F900	20.20	19.30	7.60	15
A342	59.39	60.30	16.70	14
GLF5	29.40	28.50	7.50	13
B741	70.60	59.60	19.30	13
GL5T	28.69	28.65	7.70	11
B762	48.50	47.60	15.90	11
E135	26.30	20.20	6.70	10

Table 2: Dimensions of aircraft types, along with number of records in the TSD

### 2.4 Estimating Probability of Lateral Overlap: $P_y(S_y)$

The probability of lateral overlap of aircraft nominally flying on adjacent flight paths, separated by  $S_y$ , is denoted by  $P_y(S_y)$  and is defined as

$$P_y(S_y) := \mathbf{P}(|S_y + Y_1 - Y_2| \leq \lambda_y) , \quad (2)$$

where  $Y_1$  and  $Y_2$  are assumed to be the lateral deviations of two aircraft which are nominally separated by  $S_y$ . We assume that  $Y_1$  and  $Y_2$  are identically distributed but statistically

independent with a distribution  $F_y$ . We model  $F_y$  as mixture distribution having a *core* distribution  $G_y$  and a *non-core* distribution  $H_y$ .

- The core distribution  $G_y$ , represents errors that derive from standard navigation system deviations. These errors are always present, as navigation systems are not perfect and they have a certain precision.
- The non-core distribution  $H_y$ , represents Gross Navigation Errors (GNE), that corresponds to what may be viewed as non-nominal performance.

We assume that a standard navigation system error represented by the core distribution may take large values but the non-core distribution representing gross navigation errors can only take large values. But in most cases it is impossible to determine with certainty if a given observed lateral error arose from the core or from the tail term of the distribution.

Therefore, the overall lateral deviation distribution is modeled as:

$$F_y(y) = (1 - \alpha) G_y(y) + \alpha H_y(y) \quad (3)$$

The mixing parameter  $\alpha$  is the probability of a *gross navigational error*. The core lateral deviation distribution  $G_y$  is modelled by *Double Exponential* distribution with a parameter  $\beta_y > 0$  as the rate, that is, if then

$$Y_1 \sim G_1$$

$$\mathbf{P}(|Y_1| > y) = e^{-\beta_y y},$$

where  $y \geq 0$ . In other words we assume that the core distribution has a density of the form

$$g_y(y) = \frac{\beta_y}{2} e^{-\beta_y |y|}.$$

Finally the non-core distribution  $H_y$  is modeled by a “*Separated Double Exponential*” distribution with parameters  $\mu_y > 0$ , representing the “separation and  $\gamma_y > 0$  the rate parameter, that is, if  $Y_2 \sim H_y$  then

$$\mathbf{P}(Y_2 > \mu_y + y) = \frac{1}{2} e^{-\gamma_y y} \quad \text{and}$$

$$\mathbf{P}(Y_2 < -\mu_y - y) = \frac{1}{2} e^{\gamma_y y},$$

where  $y \geq 0$ . This really means that the non-core distribution  $H_y$  gives no mass in and  $[-\mu_y, \mu_y]$  outside it decays as a Double Exponential distribution with rate parameter  $\gamma_y$ . The density of this distribution is given by

$$h_y(y) = \begin{cases} \frac{\gamma_y}{2} e^{\gamma_y(y+\mu_y)} & \text{if } y < -\mu_y \\ 0 & \text{if } -\mu_y \leq y \leq \mu_y \\ \frac{\gamma_y}{2} e^{-\gamma_y(y-\mu_y)} & \text{if } y > \mu_y \end{cases}$$

This modelling is similar to what has been used by FAA and also in EUR/SAM except here we take a double exponential distribution, namely the core distribution to explain all the typical and atypical errors which are not a gross navigational error, and use the separated double exponential distribution for the gross navigational errors. This in turn gives a better understanding of the mixing parameter  $\alpha$  which we estimate by taking the 95% *upper confidence limit* from the July 2010 - August 2011 GNE data as provided by AAI. The formula comes out to be

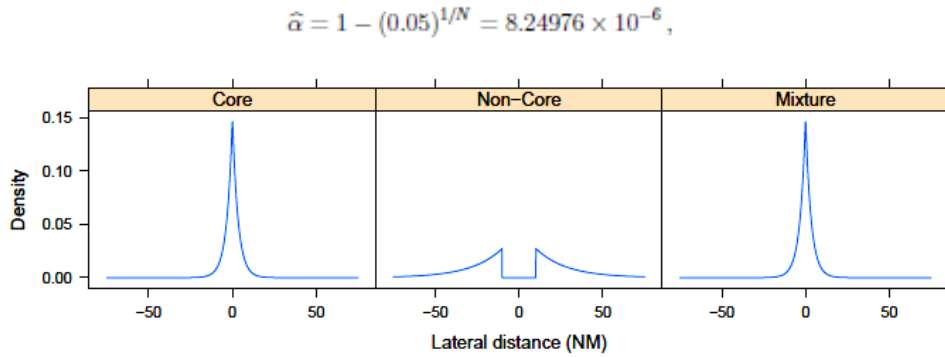


Figure 2: Modeling of lateral deviation.

Where  $N = 363128$  is the number of flights observed and no gross navigational errors were detected. More GNE data with no detected gross navigational error will increase the value of  $N$  and hence decrease the value of  $\alpha$  which will lead to decrease in the risk. Here we would like to note that even though the non-core distribution  $H_y$  has a discontinuous density  $h_y$ , it does not create difficulty in this risk assessment. The parameter  $\beta_y$  is estimated under the RNP10 assumption of  $\pm 10$  NM deviation with 95% confidence, this leads to the estimate

$$\hat{\beta}_y = -\frac{\log 0.05}{10} = 0.2995732.$$

The parameter  $\mu_y$  is taken to be 10 based on RNP10 consideration and  $\gamma_y$  is then estimated by maximizing the wingspan overlap probability with  $S_y = 50$  NM initial separation (See Figure 3). This is a conservative method similar to what has been used by FAA and also in EUR/SAM. The estimated value of  $\gamma_y$  is 0.0548971 leading to the estimated value of  $P_y(50)$  as  $3.67207 \times 10^{-8}$ . To be conservative, we also considered the possibility of unreported GNEs, and computed the estimates of  $P_y(50)$  and  $N_{ay}$  had we observed 1, 2, or 3 GNEs. The results, given below, are still well below the TLS.

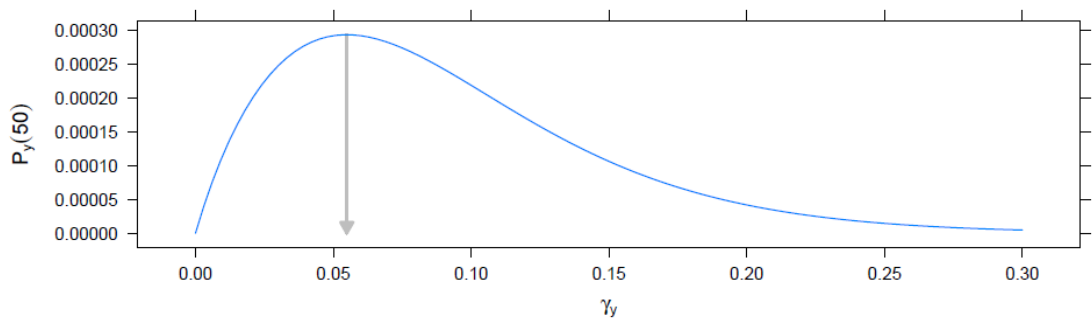


Figure 3: Wingspan overlap probability as a function of  $\gamma_y$  with  $S_y = 50$  NM initial separation.

No. of GNEs	$P_y(50)$	$N_{ay}$
0	$3.67207 \times 10^{-8}$	$1.04405 \times 10^{-9}$
1	$3.93075 \times 10^{-8}$	$1.11760 \times 10^{-9}$
2	$4.17581 \times 10^{-8}$	$1.18727 \times 10^{-9}$
3	$4.39363 \times 10^{-8}$	$1.24921 \times 10^{-9}$

The estimate of  $\alpha$  does not have a nice formula when one or more GNEs are observed, but can be computed using numerical methods.



## 2.5 Estimating Probability of Vertical Overlap: $P_z(0)$

The probability of vertical overlap of aircraft nominally flying at the same flight level on laterally adjacent flight paths is denoted by  $P_z(0)$ . It is defined by

$$P_z(0) = \mathbf{P} (|Z_1 - Z_2| \leq \lambda_z) ,$$

Where  $Z_1$  and  $Z_2$  are the height deviations of two aircraft nominally flying at the same flight levels on laterally adjacent flight paths.

We assume that  $Z_1$  and  $Z_2$  are statistically independent with distribution  $F_z$ . Unlike in the computation of  $P_y(S_y)$  where we assume the lateral deviations follow a mixture distribution here we may assume that  $F_z$  is a Double Exponential distribution with parameter  $\beta_z > 0$ , that is, with density function

$$f_z(z) = \frac{\beta_z}{2} e^{-\beta_z|z|}$$

One can then estimate  $\beta_z > 0$  by

$$\hat{\beta}_z = -\frac{\log 0.05}{0.032915} = 91.0142 .$$

This is under assumption that a typical aircraft stays within  $\pm 200$  ft =  $\pm 0.032915$  NM of its assigned flight level 95% of the time. This leads to an estimated value 0.4230008 for  $P_z(0)$ . Unfortunately this analysis ignores both the effect of large height deviations (LHDs) and aircraft altimetry system errors (ASE) which are not estimable directly. So we use a conservative value of 0.538, as used by MAAR for vertical safety assessment in BOB region.

## 2.6 Estimating the Lateral Occupancy Parameters: $E_y$ (same) and $E_y$ (opp)

In equation (1) there are two occupancy terms, one for same direction occupancy  $E_y(\text{same})$  and another one for opposite direction occupancy  $E_y(\text{opp})$ . Same direction occupancy is defined as the average number of aircraft that are, in relation to a typical aircraft

- flying in the same direction as it;
- nominally flying on tracks one lateral separation standard away;
- nominally at the same flight level as it; and
- within a longitudinal segment centered on it.

The length of the longitudinal segment,  $2S_x$ , is usually considered to be the length equivalent to 20 minutes of flight resulting to a value of 160 NM. It has been verified that the relationship between  $S_x$  and the occupancy is quite linear.

A similar set of criteria can be used to define opposite direction occupancy, just replacing “flying in the same direction” by flying in the opposite direction”. Occupancy, in general, relates to the longitudinal overlap probability and can be obtained by the equation

$$E_y = \frac{2T_y}{H} ,$$

Where  $T_y$  represents the total proximity time generated in the system and  $H$  is the total flight hours generated in the system during the considered period of time. We estimate this quantity by direct estimation from time at waypoint passing using the TSD. For this we compute the number of proximate pairs by comparing the time at which an aircraft on one route passes a waypoint with the time at which another aircraft on a parallel route passes the homologous waypoint. When the difference between passing times is less than certain value, 10 minutes in this case, it is considered that there is a proximate pair in that pair of routes. Occupancy is then calculated using the following expression:

$$E_y = \frac{2n_y}{n} ,$$

where the numerator  $n_y$  is the number of proximate pairs and the denominator,  $n$ , is the total number of aircraft. The observed number of proximate pairs and the total number of flights per route pair are summarized in Table 3.

WP1	WP2	Proximate	Total
BIDEX	ORARA	14	942
IGOGU	IGREX	272	2658
NOPEK	IGOGU	216	2646
GIRNA	IDASO	228	2970
VATLA	ORARA	68	1042
IGOGU	EMRAN	4	1972
LIBDI	MEPEL	0	180
RINDA	SAGOD	70	2666
MEPEL	IBITA	82	1442
IBITA	TEBOV	438	3338
SAGOD	IBITA	36	1462
POMAN	IGAMA	812	4110
KITAL	LOTAV	38	696
OPIRA	IGAMA	186	3030
LOTAV	REXOD	38	832
ADPOP	LELIT	0	14
TOTOX	REXOD	242	2138
TOTOX	PARAR	250	3172
ADPOP	SUGID	0	2904
RASKI	PARAR	570	5014
NOBAT	SUGID	1464	7372
POMAN	ODOLI	0	1544
KITAL	ASPUX	0	126
DOGAR	ELATI	0	280
ELATI	KETIV	4	330
KETIV	SELSU	4	522
SELSU	NISOK	2	672
NISOK	NIXUL	4	554
NIXUL	TOPIN	12	806
SULTO	DUGOS	0	458
ATETA	DEMON	0	356
DEMON	BASUR	0	6
SEBLO	ANIVE	0	74
PADLA	UBKIN	2	152

Table 3: Number of laterally proximate flights per route pair, based on TSD.

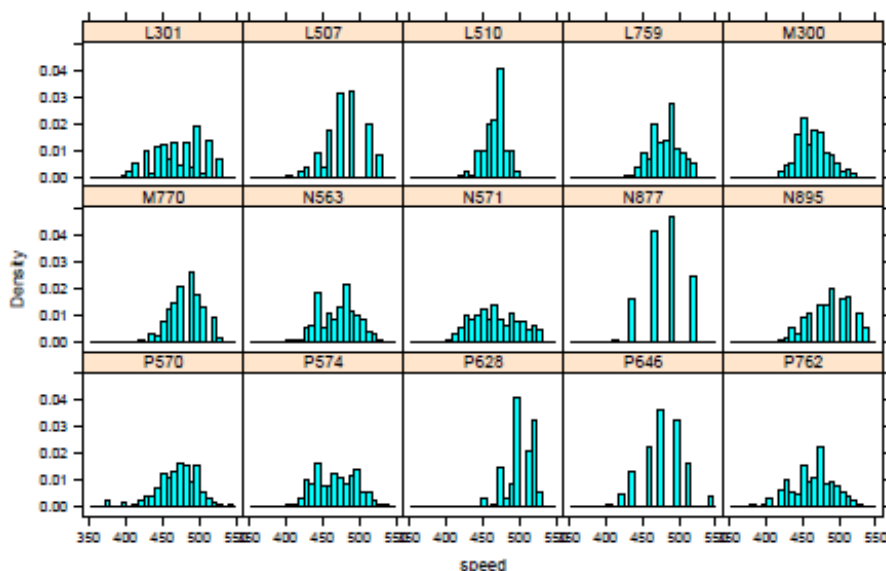


Figure 4: Distribution of estimated average speed by route.



## 2.7 Estimate of Average Ground Speed

As directly measured speed data were not provided, speeds and relative velocities have been estimated by comparing waypoint report times. To do this, we divide the distance separating the entry and exit waypoints on a route by the time taken to travel the route. The result of this operation is the speed of each aircraft. Figure 4 gives the distribution of the estimated average speed by route. We only display the RNP10 routes where RHS has been implemented.

## 2.8 Estimate of Average Relative Longitudinal Speed: $\overline{|\Delta V|}$

$\overline{|\Delta V|}$  is the average relative longitudinal speed between aircraft flying in the same direction. We estimate it from the TSD by taking the differences between the speeds of all the pairs of aircraft that constitute a lateral proximate pair in the same direction (see Figure 5).  $\overline{|\Delta V|}$  is estimated as the mean absolute value of all the calculated differences, which turns out to be 18.96988. We use the conservative value 19. Here we note that the lateral proximate pairs are already determined while estimating the parameter  $E_y(\text{same})$ .

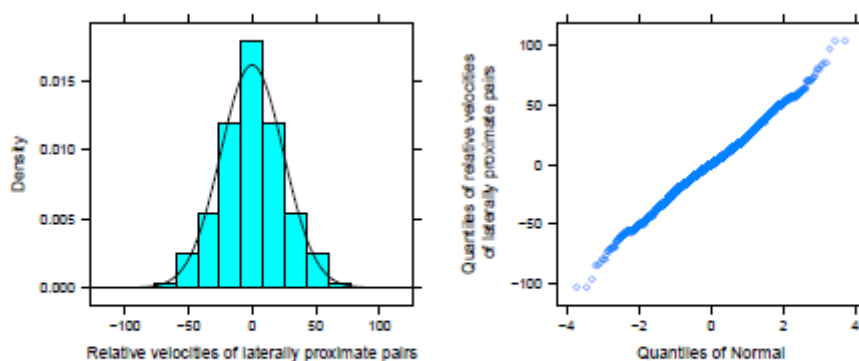


Figure 5: Distribution of relative velocities of laterally proximate pairs. The Normal distribution with sample standard deviation looks like a reasonable fit.

## 2.9 Estimate of Average Relative Lateral Speed: $\overline{|\dot{y}(S_y)|}$

$\overline{|\dot{y}(S_y)|}$  is the average relative lateral cross-track speed between aircraft, flying on adjacent routes separated by  $S_y$  NM at the same flight level, that have lost their lateral separation. The estimation of this parameter generally involves the extrapolation of radar data, speeds and lateral deviations, but such radar data were not available for this study. So we take a conservative value 75 knots as per the EMA Handbook.

## 2.10 Estimate of Average Relative Vertical Speed: $\overline{|\dot{z}|}$

$\overline{|\dot{z}|}$  denotes the average modulus of the relative vertical speed between a pair of aircraft on the same flight level of adjacent tracks that has lost lateral separation. It is generally assumed that  $\overline{|\dot{z}|}$  is independent of the size of the lateral separation between the aircraft and, for aircraft in level flight, it can also be considered that there is no dependency of  $\overline{|\dot{z}|}$  with the vertical separation between the aircraft. As noted by various agencies data on  $\overline{|\dot{z}|}$  are relatively scarce but typically taken as 1.5 knots which is considered to be conservative (see EMA Handbook).

## 3. Longitudinal Collision Risk Assessment

In order to compute the level of safety for longitudinal deviations of operations on the BOBASIO region we use the Longitudinal Collision Risk Model. It models the longitudinal collision risk due to the loss of longitudinal separation between aircraft flying on the same route at the same flight level.

The model is as follows:

$$N_{ax} = P_y(0) P_z(0) \frac{2\lambda_x}{|\dot{x}|} \left( \frac{|\dot{x}|}{2\lambda_x} + \frac{|\dot{y}(0)|}{2\lambda_y} + \frac{|\dot{z}|}{2\lambda_z} \right) \times \left[ \sum_{k=m}^M 2Q(k) P(K > k) \right]. \quad (4)$$

We would like to note that the same model has been used for the safety assessment study of the South China Sea which was carried out by SEASMA.

The parameters in the equation (4) are defined as follows:

- $N_{ax}$  := Expected number of fatal accidents (two for every collision) per flight hour due to the loss of longitudinal separation between co-altitude aircraft flying on the same track with planned minimum  $m$  NM longitudinal separation.
- $m$  := Minimum longitudinal separation in NM.
- $M$  := Maximum initial longitudinal separation between aircraft pair which will be monitored by ATC in order to prevent loss of longitudinal separation standard.
- $\lambda_x$  := Average length of an aircraft flying in BOBASIO region.
- $\lambda_y$  := Average wingspan of an aircraft flying in BOBASIO region.
- $\lambda_z$  := Average height of an aircraft flying in BOBASIO region.
- $P_y(0)$  := Probability of lateral overlap of aircraft assigned at the same route and flight level .
- $P_z(0)$  := Probability of vertical overlap of aircraft assigned at the same flight path at the same flight level .
- $|\dot{x}|$  := Minimum relative along-track speed necessary for following aircraft in a pair separated by  $m$  NM at a reporting point to overtake lead aircraft at the next reporting point.
- $|\dot{y}(0)|$  := Relative across-track speed of same route aircraft pair.
- $|\dot{z}|$  := Average relative vertical speed of a co-altitude aircraft pair assigned to the same route.
- $Q(k)$  := Proportion of aircraft for which the following aircraft has initial longitudinal separation  $k$ .
- $P(K > k)$  := Probability that a pair of same route co-altitude aircraft with initial longitudinal separation  $k$  will lose at least as much as  $k$  longitudinal separation before correction by ATC. Once again, a collision, and consequently two fatal accidents, can only occur if there is overlap between two aircraft in all three dimensions simultaneously. Equation (4) gathers the product of the probabilities of losing separation in each one of the three dimensions. The equation is derived under similar assumption as done in the case of lateral collision risk assessment.

We should note here the first part of the right-hand side of the equation (4) gives the probability of a collision given an event of overtake of a front aircraft by a behind aircraft when both are nominally flying at the same route at the same flight level, and the second part which is inside the square bracket is the expected number of aircraft involved in such overtake events.

### 3.1 Estimated Values of the Parameters and Estimated Longitudinal Collision Risk

The following table gives the values of the parameters of the right-hand side of the equation (4) which are obtained from our analysis

Parameter	Estimated Values	Source of the Estimate
$m$	50 NM	Current minimum longitudinal separation (due to Phase 1 RHS).
$M$	160 NM	Conservative value corresponding to 20 minutes separation.
$\lambda_x$	0.04065875 NM	Estimated from TSD (See Section 2.3).
$\lambda_y$	0.04308855 NM	Estimated from TSD (see Section 2.3).
$\lambda_z$	0.01301296 NM	Estimated from TSD (see Section 2.3).
$P_y(0)$	0.2	Conservative estimate (see Section 3.2).
$P_z(0)$	0.538	Conservative value used in previous safety assessments (see Section 2.5).
$ \dot{x} $	50 knots	Conservative estimate using speed and distance between way points (see Section 3.3).
$ \dot{y}(0) $	1 knot	RASMAG/9 safety assessment (see Section 3.4).
$ \dot{z} $	1.5	Conservative value as per EMA Handbook (see Section 2.10).
$Q(k)$	See Table 4	Obtained from TSD (see Section 3.5).
$P(K > k)$	See Table 4	Computed using normal model on speed (see Section 3.6).

Finally this leads to the following estimate for the longitudinal collision risk  $N_{ax}$ .

$$N_{ax} = 6.7326 \times 10^{-10}$$

It is worth noting that this risk estimate is significantly lower than the one we obtained in earlier occasions of analyzing TSD of December 2010 and TSD of August 2011. The estimate has been better and hence projecting a much lower risk than what was estimated earlier, because this time we have a much larger data set and so we have been able to do better fitting of the model.

$k$ (mins)	$k$ (NM)	$Q(k)$	$P(K > k)$
7	56	0.0001765069	$1.40443 \times 10^{-5}$
8	64	0.0003530139	$9.12675 \times 10^{-7}$
9	72	0.0002206337	$4.24022 \times 10^{-8}$
10	80	0.0007942812	$1.40523 \times 10^{-9}$
11	88	0.0094431206	$3.31628 \times 10^{-11}$
12	96	0.0091342335	$5.56579 \times 10^{-13}$
13	104	0.0083840791	$6.62902 \times 10^{-15}$
14	112	0.0102815285	$8.60912 \times 10^{-17}$
15	120	0.0098843880	0
16	128	0.0107227959	0
17	136	0.0102815285	0
18	144	0.0091783603	0
19	152	0.0102815285	0
20	160	0.0102374018	0

Table 4: Estimated values of  $Q(k)$  and  $P(K > k)$

### 3.2 Estimating Probability of Lateral Overlap: $P_y(0)$

$P_y(0)$  is defined as the probability of lateral overlap of aircraft nominally flying at adjacent flight levels on same route. We can now use the same mixture model of Section 2.4 to compute this parameter by substituting  $S_y = 0$  in the equation (2). This leads to an estimate of  $P_y(0)$  as 0.2.

However as noted earlier in the EUR/SAM report, this factor  $P_y(0)$  has a significant effect on the risk estimate. Therefore, it should not be underestimated.  $P_y(0)$  will increase as the lateral navigational performance of typical aircraft improves, causing a corresponding increase in the collision risk estimate. As reported in the EUR/SAM report, the RGCSP was aware of this problem and attempted to account for improvements in navigation systems when defining the RVSM global system performance specification. Based on the performance of highly accurate area navigation systems observed in European airspace, which demonstrated lateral path-keeping errors with a standard deviation of 0.3 NM, the RGCSP adopted a value of 0.059 as the value of  $P_y(0)$  for the global system performance. We further note that in the EMA Handbook the value has been taken conservatively as 0.2. We take this rather conservative value for our analysis as well.

### 3.3 Estimation of the Parameter $|\dot{x}|$

$|\dot{x}|$  is defined as the minimum relative along-track speed necessary for following aircraft in a pair separated by  $m$  NM at a reporting point to overtake lead aircraft at the next reporting point. Thus if  $d$  is the distance between the two way points and  $v_0$  is the speed of the front aircraft, then  $|\dot{x}|$  can be computed by the following equation

$$\frac{d - m}{v_0} = \frac{d}{v_0 + |\dot{x}|},$$

leading to

$$|\dot{x}| = \frac{mv_0}{d - m}.$$

We conservatively estimate it by taking  $v_0$  as the minimum speed observed in TSD which is 360 NM per hour and the maximum distance between two waypoints on the routes which we study which is  $d = 404$  NM. With  $m = 50$  NM the final estimate turns out to be  $|\dot{x}| = 50.847$  knots. We use a conservative value of 50 knots.

### 3.4 Estimation of the Parameter $|\dot{y}(0)|$

$|\dot{y}(0)|$  is defined as the relative cross-track speed of same route aircraft pair. No data is available for estimation of this parameter so we take a conservative value of 1 knot as given in the EMA Handbook.

### 3.5 Estimation of the Parameter $Q(k)$

$Q(k)$  is defined as the proportion of aircraft pairs with initial longitudinal separation  $k$ . We estimate its value from the TSD. Flights entering the FIR on different routes and assigned different flight levels were considered separately (see Figure 6), and the waiting times between successive arrivals were tabulated in minutes. We assume an average speed of 8 NM per minute, and compute the proportion  $Q(k)$  as

$$Q(k) = \frac{\text{number of flight pairs with inter-arrival distance } 8k}{\text{total number of flight pairs with at least 80 NM separation}}.$$

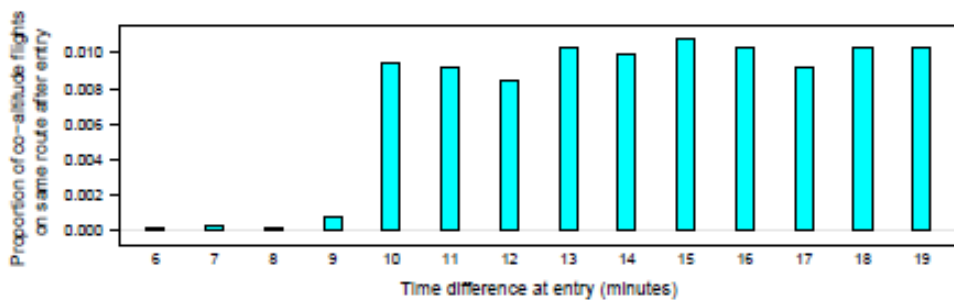


Figure 6: Values of  $Q(k)$  estimated from TSD. For co-altitude flights on the same route (after entry / before exit), the proportion of flights that entered  $k$  minutes after the preceding flight is plotted for  $k = 7, 8, 9, \dots, 20$  minutes.

The final estimated values of  $Q(k)$  for  $k$  ranging between 6 and 20 minutes is given in the Table 4.

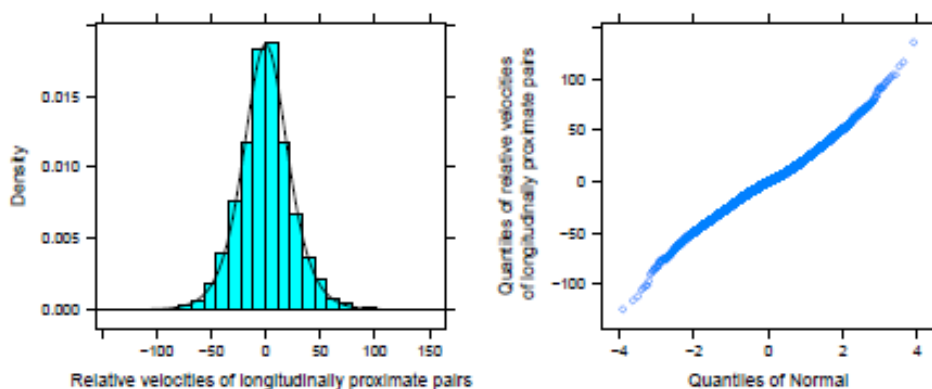


Figure 7: Distribution of relative velocities of longitudinally proximate pairs. The Normal distribution does not necessarily seem to be a reasonable fit.

### 3.6 Estimation of the Parameter $P(K > k)$

To estimate  $P(K > k)$  we consider two aircraft flying on same route at same flight levels at the same direction. Let  $V$  and  $V'$  be their ground speeds of the front and behind aircraft respectively. We assume these speeds to be statistically independent but identically distributed. Let  $T_0$  be the maximum duration of time before ATC intervenes. Then

$$P(K > k) = P\left(0 < \frac{k}{V' - V} < T_0\right) = P\left(V' - V > \frac{k}{T_0}\right).$$

We note here that the value of  $T_0$  is conservatively taken to be 0.5 hours. Now we finally estimate these probabilities using the TSD. For that we consider the difference in velocity of two aircraft nominally flying on the same route at the same flight level. We conservatively consider velocity differences of all flight pairs which are separated by 2 hours time at entry. It is to be noted that we observed from the TSD data that two hours is more than the maximum time taken by any aircraft to travel between its entry and exit points. We observe that these differences in velocity are symmetrically distributed around zero but from the histogram and the quantile-quantile plot (see Figure 7) it is not clear that these differences necessarily normally distributed. Though unlike in the previous analysis of December 2010 and August 2011 data sets this time the plot is more of a straight line than not. Still to be conservative, this time we postulate the following mixture model for the density of these velocity differences.

$$f_v(v) = p \frac{1}{\sqrt{2\pi}\tau_v} e^{-\frac{v^2}{2\tau_v^2}} + (1-p) \frac{1}{\sqrt{2\pi}\sigma_v} e^{-\frac{v^2}{2\sigma_v^2}},$$

which is a mixture of two zero-centered Normal densities with different standard deviations, namely,  $\tau_v$  and  $\sigma_v$  and mixing proportion  $p$ . This somewhat different than the one we proposed in the earlier analysis where a mixture of normal and double exponential were postulated. This time it turned out that such a mixture is not a good fit for the velocity difference. This is perhaps because now we have a larger data set consisting of all the Indian FIRs and Colombo FIR and considered all the RNP10 routes. It is typical in statistics a larger data set gives better model fitting.

We now estimate the parameters of this mixture model by their maximum likelihood estimates (MLEs). Since this is a mixture model so we use the Expectation-Maximization (EM) algorithm to find the MLEs. The algorithm converged rapidly to give the following estimates:

$$\hat{p} = 0.2245596, \hat{\tau}_v = 9.581999, \text{ and } \hat{\sigma}_v = 27.11642.$$

It is well known in Statistics literature that even though the EM algorithm increases the value of the likelihood it may get trapped in a local maximum. To avoid this problem we tried several starting values and observed that the algorithm always converges to the same estimated values given above.

So it is statistically reasonable to accept the mixing density with this value of the parameters as a good estimate of the true density of the velocity differences. A graphical representation of the fit is given in Figure 8.

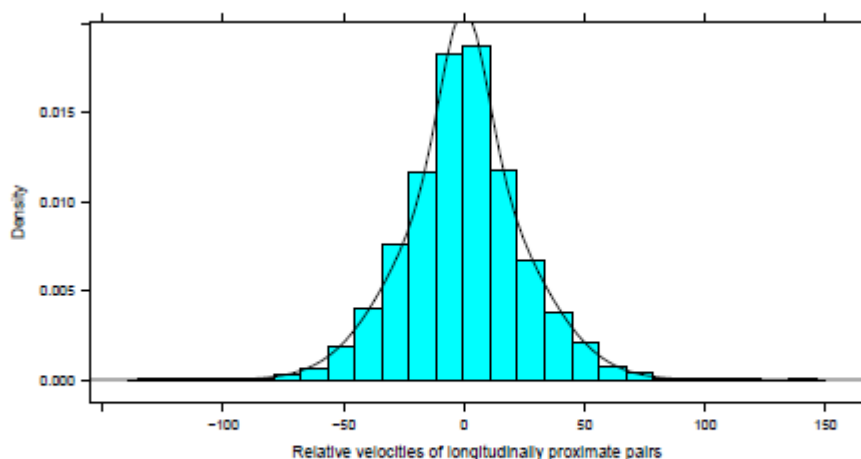


Figure 8: Distribution of relative velocities of laterally proximate pairs along with estimated mixture density (estimated using the EM algorithm).

With these we estimate the values of  $P(K > k)$  for  $k$  ranging between 7 and 20. These are presented in the Table 4

#### 4. Summary of the Safety Assessment

The following table gives a summary of the safety assessment of the BOBASIO region for the month of December 2011.

Type of Risk	Estimated Risk	TLS	Remarks
Lateral Risk	$1.04405 \times 10^{-9}$	$5 \times 10^{-9}$	Below TLS
Longitudinal Risk	$0.67326 \times 10^{-9}$	$5 \times 10^{-9}$	Below TLS

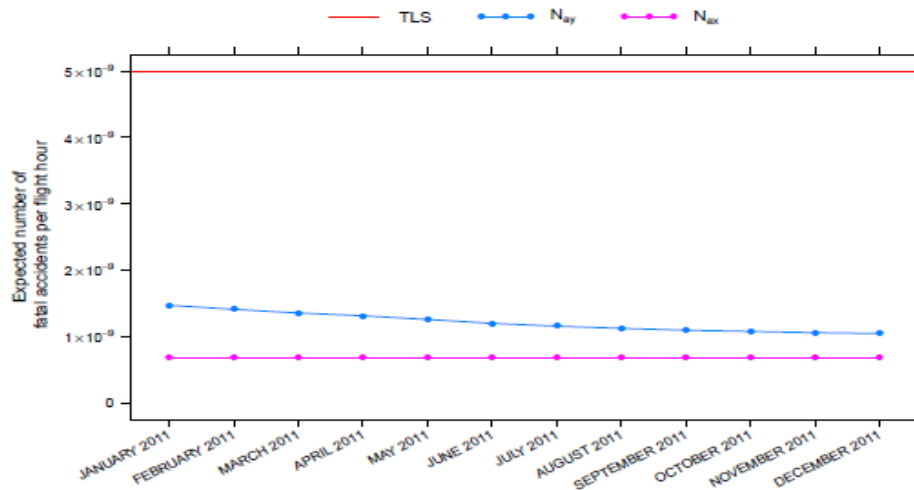


Figure 9: Assessment of Compliance with Lateral and Longitudinal TLS Values.

Figure 9 presents the results of the collision risk estimates for each month using the cumulative 12-month LLD and LLE reports since January 2011.